Fundamental Solutions in Multiphase Geo-Poro-Mechanics for the Analysis of Seismic Site Effects

Pooneh Maghoul

Université Paris-Est, Laboratoire Navier (UMR CNRS 8205)

École des Ponts ParisTech

PhD Advisors:

Behrouz Gatmiri, Denis Duhamel

1. **Unsaturated soils**
   - General context and fields of application
   - Basic assumptions
   - Governing equations
2. **Boundary element method**
   - Problematics
   - Fundamental Solution
   - Boundary Integral Equation
   - Discretization
3. **Implementation in « HYBRID » FEM/BEM code**
   - Programming
   - Validation
4. **Applications in seismic site effects**
   - Introduction
   - Topographic site effects in 2D configurations
   - Combined effects in fully-filled alluvial valleys
   - Alluvial effect in a partially-filled valley
5. **Conclusion and Perspective**

1 **Unsaturated soils**
- General context and fields of application
- Basic assumptions
- Governing equations

2 Boundary element method
- Problematics
- Fundamental Solution
- Boundary Integral Equation
- Discretization

3 Implementation in « HYBRID » FEM/BEM code
- Programming
- Validation

4 Applications in seismic site effects
- Introduction
- Topographic site effects in 2D configurations
- Combined effects in fully-filled alluvial valleys
- Alluvial effect in a partially-filled valley

5 Conclusion and Perspective

Unsaturated soils: Multiphase media

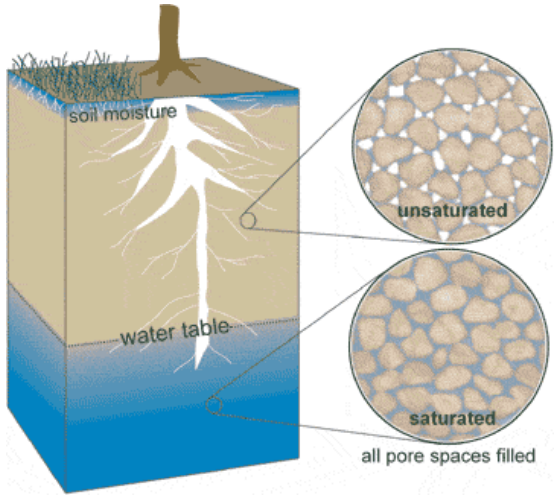

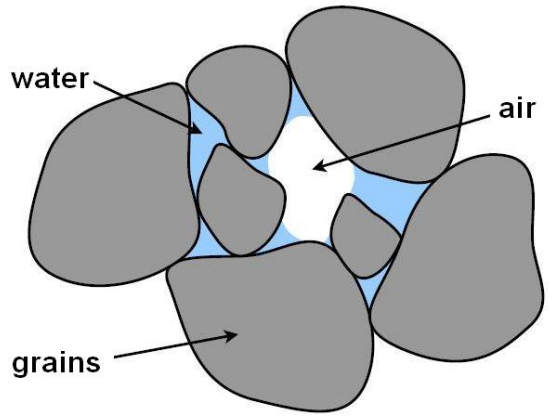

An unsaturated porous medium is represented as a three-phase system:

- Deformable solid skeleton
- Water
- Air

Theoretical background on unsaturated porous media

Behaviour laws in unsaturated soils

- ***Formulation:***
  Bishop's effective stress [Bishop & Donald 1961, Bishop & Blight 1963],

$$\sigma'_{ij} = \sigma_{ij} - \underbrace{(\chi p_w + (1-\chi)p_a)}_{p^*}\delta_{ij}$$

  Independent state variables [Matyas & Radhakrishna 1968, Fredlund & Morgernstern 1977, Gens et al. 1998]

$$\left.\begin{array}{lll} (\sigma_{ij} - p_a\delta_{ij}) & , & (p_a - p_w)\delta_{ij} \\ (\sigma_{ij} - p_w\delta_{ij}) & , & (p_a - p_w)\delta_{ij} \\ (\sigma_{ij} - p_a\delta_{ij}) & , & (\sigma_{ij} - p_w\delta_{ij}) \end{array}\right\} \Rightarrow \dot{\varepsilon}_{ij} = \dot{\varepsilon}^m_{ij} + \dot{\varepsilon}^h_{ij}$$

- ***State surface models***
  [Matyas & Radhakrishna 1968, Fredlund & Morgenstern 1976, Fredlund 1979, Lloret and Alonso 1985, Edgar et al. 1989, Gatmiri 1997, Gatmiri & Delage 1995]
  Two volume-mass constitutive relations have to be formulated and combined to link all of the properties related to the mass and the volume of soil to the stress state variables.

$$(e, \theta_w); (e, S_r)$$

Theoretical background on unsaturated porous media

Thermal effects in unsaturated soils

- ***Experimental studies***
  [Romero 1999, Kanno et al. 1999, Chijimatsu et al. 2000]
- ***Humidity transfer modelling***
  [Rollins et al. 1954, Philip and de Vries 1957, de Vries 1958, Dakshanamurthy and Fredlund 1981]
- ***Heat flow***
  [Lemaître and Chaboche 1985, Farouki 1986, Wilson 1990]
- ***Fully coupled behaviour law***
  Unique relationship between the saturation degree and the independent state variables [Taylor & Cary 1964, Matyas and Radhakrishna 1968] ,
  Volumetric effects on the solid skeleton [Geraminezad and Saxena 1986],
  Multi-phase model without vapour [Schrefler et al. 1995],
  Fully-coupled models [Thomas & King 1991, Thomas & He 1995, Gens et al. 1997, Gatmiri & Delage 1995, Gatmiri 1997, Gatmiri et al. 1998, Gatmiri 2000, Gatmiri & Arson 2008]

Wave propagation in unsaturated soils

- ***Dynamic modelling***
  Zienkiewicz et al. (1990) Based on the Bishop formulation
  Muraleetharan & Wei (1999) Using the theory of mixtures with interfaces (TMI) based on the two stress state variables,
  Many unknown constitutive parameters that are extremely difficult to assess!

Constitutive assumptions

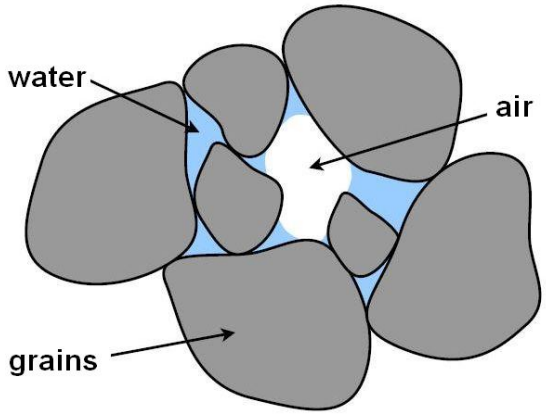

- Set of fully coupled governing differential equations:
  poromechanics theory + suction-based mathematical model Gatmiri (1997)
- Micromechanical phenomena $\Rightarrow$ Macroscopic level $\Rightarrow$ Multiscale formulations
- **Porosity** and **Degree of saturation** with respect to $\alpha\,(= w, a)$:

$$n = \frac{V_{pores}}{V_{tot}} \quad \& \quad S_\alpha = \frac{V^\alpha_{pores}}{V_{pores}} = \frac{n_\alpha}{n} \quad \Rightarrow \quad \sum_\alpha S_\alpha = 1 \quad \& \quad n = \sum_\alpha n S_\alpha$$

Constitutive assumptions

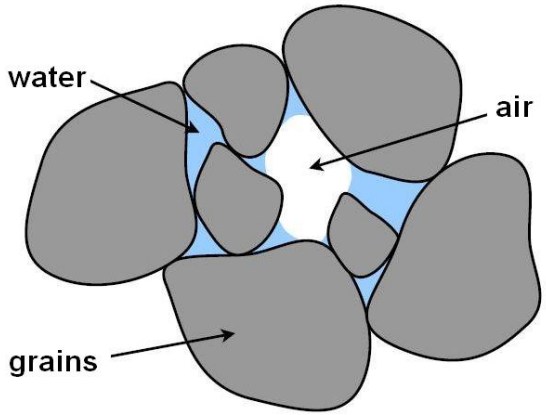

Displacement field

- Displacement of the solid skeleton: $\mathbf{u}$
- Displacement of the fluid α relative to the solid: $\mathbf{w}^{\alpha}$
- Absolute displacements of the fluid α: $\mathbf{U}^{\alpha}$

Velocity field

- Velocity of the solid skeleton: $\dot{\mathbf{u}}$
- Absolute velocity of the fluid α: $\dot{\mathbf{U}}^{\alpha}$
- Relative flow vector of fluid volume (with respect to the skeleton) or Darcy flow velocity for α: $\dot{\mathbf{w}}^{\alpha} = nS_{\alpha}(\dot{\mathbf{U}}^{\alpha} - \dot{\mathbf{u}})$

Constitutive assumptions

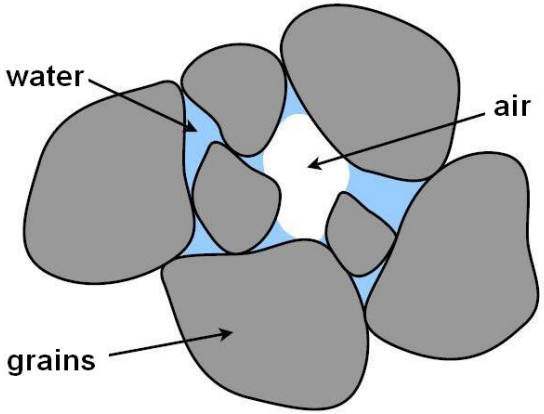

- **Stress state variables**

Net stress: $(\sigma_{ij} - p_a \delta_{ij})$

Suction: $(p_a - p_w)$

Governing equations for solid skeleton

- Dynamic equilibrium equation for the mixture using total net stress

$$\left(\sigma_{ij} - \delta_{ij} p_a\right)_{,j} + p_{a,i} + f_i = \rho \ddot{u}_i$$

- Constitutive law [Gatmiri et al. 1997, Gatmiri & Hoor, 2007]:
  stress-suction-strain relation which considers the effect of suction on deformation

$$d\left(\sigma_{ij} - \delta_{ij} p_a\right) = D_{ijkl}\, d\varepsilon_{kl} - F^s \delta_{ij}\, d\left(p_a - p_w\right)$$

- Linear strain-displacement relation, i.e., assuming small deformation gradients:

$$\varepsilon_{ij} = \left(u_{i,j} + u_{j,i}\right)/2$$

Nomenclature

$\rho = \rho_s(1-n) + \rho_w n_w + \rho_a n_a$: Bulk density

f_i: Bulk body force

D_{ijkl}: Linear elastic stiffness tensor

$F^s \delta_{ij} = D_{ijkl} (D^{suc}_{lk})^{-1}$

$(D^{suc}_{lk})^{-1} = \beta_{suc} [1,1,0]^T, \beta_{suc} = \dfrac{1}{1+e} \dfrac{\partial e}{\partial (p_a - p_w)}$

$e = f(\sigma - p_a, p_a - p_w)$: Void ratio

Governing equations for solid skeleton

- Dynamic equilibrium equation for the mixture using total net stress

$$\left(\sigma_{ij} - \delta_{ij} p_a\right)_{,j} + p_{a,i} + f_i = \rho \ddot{u}_i$$

- Constitutive law [Gatmiri et al. 1997, Gatmiri & Hoor, 2007]:
  stress-suction-strain relation which considers the effect of suction on deformation

$$d\left(\sigma_{ij} - \delta_{ij} p_a\right) = D_{ijkl}\, d\varepsilon_{kl} - F^s \delta_{ij}\, d\left(p_a - p_w\right)$$

- Linear strain-displacement relation, i.e., assuming small deformation gradients:

$$\varepsilon_{ij} = \left(u_{i,j} + u_{j,i}\right)/2$$

$$(\lambda + \mu) u_{\beta,\alpha\beta} + \mu u_{\alpha,\beta\beta} + F^s p_{w,\alpha} + (1 - F^s) p_{a,\alpha} - \rho \ddot{u}_\alpha + f_\alpha = 0$$

Governing equations for water

- Water mass conservation:

$$\dot{w}^w_{i,i} = -S_w \dot{\varepsilon}_{ii} + C_{ww} \dot{p_w} + C_{wa} \dot{p_a}$$

- Water transfer equation:

$$-p_{w,i} = \rho_w \ddot{\mathbf{u}} + \frac{\dot{\mathbf{w}}^w}{k_w}$$

$$-S_w \dot{u}_{\alpha,\alpha} + \rho_w k_w \ddot{u}_{\alpha,\alpha} + k_w p_{w,\alpha\alpha} + C_{ww} \dot{p_w} + C_{wa} \dot{p_a} = 0$$

Nomenclature

$\dot{w}^w_i$: Relative flow vector of fluid volume (with respect to the skeleton) or Darcy flow velocity for water

$C_{ww} = (n g_1 - C_w n S_w)$ $\quad$ $g_1 = dS_w/d(p_a - p_w)$ $\quad$ k_w: Water permeability

$C_{wa} = C_{aw} = -n g_1$ $\quad$ $C_w = (d\rho_w/\rho_w)/dp_w$: Water compressibility

Governing equations for air

- Air mass conservation:

$$\dot{w}^a_{i,i} = -S_a \dot{\varepsilon}_{ii} + C_{wa} \dot{p_w} + C_{aa} \dot{p_a}$$

- Air transfer equation:

$$-p_{a,i} = \rho_a \ddot{\mathbf{u}} + \frac{\dot{\mathbf{w}}^a}{k_a}$$

$$-S_a \dot{u}_{\alpha,\alpha} + \rho_a k_a \ddot{u}_{\alpha,\alpha} + k_a p_{a,\alpha\alpha} + C_{wa} \dot{p_w} + C_{aa} \dot{p_a} = 0$$

Nomenclature

$\dot{w}^a_i$: Relative flow vector of fluid volume (with respect to the skeleton) or Darcy flow velocity for air

$C_{aa} = (n g_1 - C_a n S_a)$ $\quad g_1 = dS_w/d(p_a - p_w)$ $\quad k_a$: Air permeability

$C_{wa} = C_{aw} = -n g_1$ $\quad C_a = (d\rho_a/\rho_a)/dp_a$: Air compressibility

Set of governing equations for unsaturated soils

- Representation in **Laplace transform domain**:

$$\tilde{f}(s) = \mathcal{L}\{f(x,t),s\} = \int_0^{+\infty} e^{-st} f(t)dt$$

Summary of the governing equations in Laplace transform domain

- Solid skeleton equation

$$(\lambda+\mu)\tilde{u}_{\beta,\alpha\beta} + \mu\tilde{u}_{\alpha,\beta\beta} + F^s\tilde{p}_{w,\alpha} + (1-F^s)\tilde{p}_{a,\alpha} - \rho s^2\tilde{u}_\alpha + \tilde{f}_\alpha = 0$$

- Water equation

$$-s\theta_1\tilde{u}_{\alpha,\alpha} + k_w\tilde{p}_{w,\alpha\alpha} + C_{ww}s\tilde{p}_w + C_{wa}s\tilde{p}_a = 0$$

in which $\theta_1 = (S_w - \rho_w k_w s)$

- Air equation

$$-s\theta_2\tilde{u}_{\alpha,\alpha} + C_{wa}s\tilde{p}_w + k_a\tilde{p}_{a,\alpha\alpha} + C_{aa}s\tilde{p}_a = 0$$

in which $\theta_2 = (S_a - \rho_a k_a s)$

Set of governing equations for unsaturated soils

- The transformed coupled differential equation system written into the matrix form:

$$\mathbf{B} \begin{bmatrix} \tilde{u}_\alpha \\ \tilde{p}_w \\ \tilde{p}_a \end{bmatrix} = - \begin{bmatrix} \tilde{f}_\alpha \\ 0 \\ 0 \end{bmatrix}$$

with the **not self-adjoint** differential operator **B**:

$$\mathbf{B} = \begin{bmatrix} \left(\mu\nabla^2 - \rho s^2\right)\delta_{\alpha\beta} + (\lambda+\mu)\,\partial_\alpha\partial_\beta & F^s\partial_\alpha & (1-F^s)\,\partial_\alpha \\ -s\,\theta_1\partial_\beta & k_w\nabla^2 + C_{ww}s & C_{wa}s \\ -s\,\theta_2\partial_\beta & C_{wa}s & k_a\nabla^2 + C_{aa}s \end{bmatrix}$$

1 Unsaturated soils
- General context and fields of application
- Basic assumptions
- Governing equations

2 **Boundary element method**
- Problematics
- Fundamental Solution
- Boundary Integral Equation
- Discretization

3 Implementation in « HYBRID » FEM/BEM code
- Programming
- Validation

4 Applications in seismic site effects
- Introduction
- Topographic site effects in 2D configurations
- Combined effects in fully-filled alluvial valleys
- Alluvial effect in a partially-filled valley

5 Conclusion and Perspective

Numerical method: Boundary Element Method

Advantages

- Bounded and unbounded media
- Smaller meshes and system of equations
- Wave propagation
- Outgoing waves through infinite domains, far field

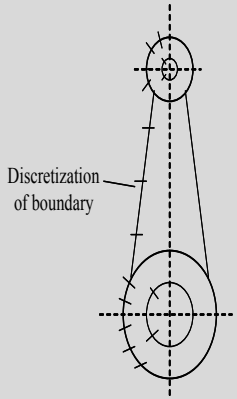

Weakness

- Analytical development (Fundamental Solution)

Principles

- Establishment of the boundary integral equations
- Derivation of the the fundamental solutions for the governing partial differential equations
- Discretization by boundary elements

Definition

Mathematical definition

- Solution of a system of partial differential equations due to a concentrated source:

$$\mathcal{L}\left[G(x,\xi,t,\tau)\right] = \delta(x-\xi)\delta(t-\tau)$$

$$\mathcal{L}\left[G(x,\xi,t,\tau)\right] = \delta(x-\xi)H(t-\tau)$$

Physical interpretation

- Potential function $\Pi(x,\xi)$ or response of the medium in the point x to a point excitation $e(\xi)$ in a domain with infinite boundaries which is a Dirac delta function in space and either a Dirac delta function or Heaviside step function in time.

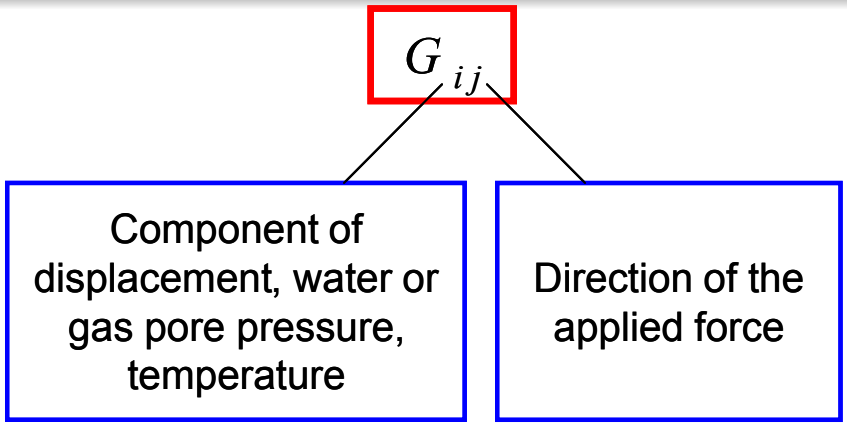

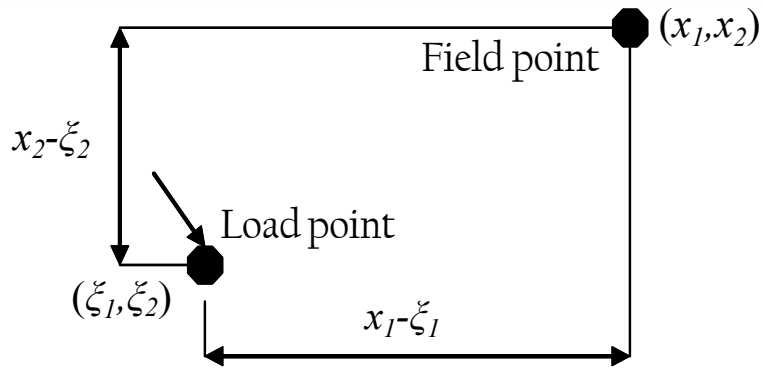

Fundamental solutions for unsaturated soils

	Problem	Domain	Dimension	Reference
Gatmiri & Jabbari (2004)	static HHM	time-independent	2D & 3D	**BeTeq Conference**
Gatmiri & Jabbari (2005)	transient HHM	time & Laplace	2D & 3D	**IJSS** 42
Jabbari & Gatmiri (2007)	static THHM	time-independent	2D & 3D	**CMES** 18(1)
Maghoul, Gatmiri & Duhamel (2010)	transient HHM	Laplace	2D	**BeTeq Conference**
Gatmiri & **Maghoul** Duhamel (2010)	transient THHM	time & Laplace	2D	**IJSS** 47
Maghoul, Gatmiri & Duhamel (2010)	transient THHM	time & Laplace	3D	**IJNAMG** 34
Maghoul, Gatmiri & Duhamel (2010)	dynamic HHM	Laplace	2D	**SDEE** in press
Maghoul, Gatmiri & Duhamel (2010)	dynamic HHM	Laplace	3D	**ECCM Conference**

HHM $\rightsquigarrow$ Hydro-mechanical model
THHM $\rightsquigarrow$ Thermo-hydro-mechanical model

Method of Hörmander (1963)

- Definition of fundamental solutions:

$$\tilde{\mathbf{B}}(\partial x, s)\tilde{\mathbf{G}}(\partial x, s) + \mathbf{I}\delta(x - \xi) = \mathbf{0}$$

- Definition of matrix of cofactors:

$$\tilde{\mathbf{B}}\tilde{\mathbf{B}}^{co} = \mathbf{I}\det(\tilde{\mathbf{B}})$$

- If a potential function exists:

$$\det(\tilde{\mathbf{B}})\varphi + \delta(x - \xi) = 0$$

- Fundamental solution is obtained by:

$$\tilde{\mathbf{G}}(\partial x, s) = \tilde{\mathbf{B}}^{co}\varphi$$

2D Dynamic Fundamental Solutions for Unsaturated Soils

- Using the adjoint operator $\Rightarrow$ $\tilde{\mathbf{B}}^{\star}\tilde{\mathbf{G}} + \mathbf{I}\delta(x-\xi) = \mathbf{0}$

$$\mathbf{B}^{\star} = \begin{bmatrix} \left(\mu\nabla^2 - \rho s^2\right)\delta_{\alpha\beta} + (\lambda+\mu)\,\partial_\alpha\partial_\beta & s(S_w - \rho_w k_w s)\partial_\alpha & s(S_a - \rho_a k_a s)\partial_\alpha \\ -F^s\partial_\beta & k_w\nabla^2 + C_{ww}s & C_{wa}s \\ -(1-F^s)\,\partial_\beta & C_{wa}s & k_a\nabla^2 + C_{aa}s \end{bmatrix}$$

- The determinant is written:

$$\det(\mathbf{B}^{\star}) = \mu(\lambda+2\mu)\,k_w k_a \left(\nabla^2 - \lambda_1^2\right)\left(\nabla^2 - \lambda_2^2\right)\left(\nabla^2 - \lambda_3^2\right)\left(\nabla^2 - \lambda_4^2\right)$$

2D Dynamic Fundamental Solutions for Unsaturated Soils

- The determinant is written:

$$\det\left(\mathbf{B}^{\star}\right) = \mu\left(\lambda + 2\mu\right) k_w k_a \left(\nabla^2 - \lambda_1^2\right)\left(\nabla^2 - \lambda_2^2\right)\left(\nabla^2 - \lambda_3^2\right)\left(\nabla^2 - \lambda_4^2\right)$$

with the roots

$\lambda_1^2 = \rho s^2/\mu \rightsquigarrow$ Related to the shear wave velocity propagating through the medium

$\lambda_2^2, \lambda_3^2, \lambda_4^2 \rightsquigarrow$ These three roots correspond to the three compressional waves which are affected by the degree of saturation and the spatial distribution of fluids within the medium.
When the pore space is filled with two immiscible fluids, capillary forces are important and the existence of a third compressional wave (i.e., a second slow wave) is predicted in the medium

[Wei & Muraleetharan 2002, Ashayeri et al. 2010].

2D Dynamic Fundamental Solutions for Unsaturated Soils

$$\lambda_2^2+\lambda_3^2+\lambda_4^2 = \frac{\rho s^2}{(\lambda+2\mu)} + \frac{F^s\rho_w s^2}{(\lambda+2\mu)} + \frac{\rho_a(1-F^s)s^2}{(\lambda+2\mu)} - \frac{C_{aa}s}{k_a} - \frac{C_{ww}s}{k_w} - \frac{S_w F^s s}{(\lambda+2\mu)k_w} - \frac{S_a(1-F^s)s}{(\lambda+2\mu)k_a}$$

$$\begin{aligned}\lambda_2^2\lambda_3^2+\lambda_2^2\lambda_4^2+\lambda_3^2\lambda_4^2 = & -\frac{\rho C_{aa}s^3}{(\lambda+2\mu)k_a} - \frac{\rho C_{ww}s^3}{(\lambda+2\mu)k_w} - \frac{\rho_w(F^sC_{aa}-(1-F^s)C_{wa})s^3}{(\lambda+2\mu)k_a} \\ & - \frac{\rho_a(-F^sC_{wa}+(1-F^s)C_{ww})s^3}{(\lambda+2\mu)k_w} + \frac{(C_{ww}C_{aa}-C_{wa}^2)s^2}{k_wk_a} \\ & + \frac{S_w(F^sC_{aa}-(1-F^s)C_{wa})s^2}{(\lambda+2\mu)k_wk_a} + \frac{S_a(-F^sC_{wa}+(1-F^s)C_{ww})s^2}{(\lambda+2\mu)k_wk_a}\end{aligned}$$

$$\lambda_2^2\lambda_3^2\lambda_4^2 = \frac{\rho(C_{ww}C_{aa}-C_{wa}^2)s^4}{(\lambda+2\mu)k_wk_a}$$

2D Dynamic Fundamental Solutions for Unsat. Soils (cont.)

$\det(\tilde{\mathbf{B}})\varphi + \delta(x-\xi) = 0$ yielding

$$\det\left(\tilde{\mathbf{B}}^{\star}(\partial x, s)\right)\varphi + \delta(x-\xi) =$$

$$(\nabla^2 - \lambda_1^2)(\nabla^2 - \lambda_2^2)(\nabla^2 - \lambda_3^2)(\nabla^2 - \lambda_4^2)\underbrace{\mu\,(\lambda + 2\mu)\,k_w k_a\,\varphi}_{\Phi} + \delta(x-\xi) = 0$$

For the iterated Helmholtz operator

$(\nabla^2 - \lambda_1^2)\,\varphi_1 + \delta(x-\xi) = 0$ $\varphi_1 = (\nabla^2 - \lambda_2^2)\,(\nabla^2 - \lambda_3^2)\,(\nabla^2 - \lambda_4^2)\,\Phi$	$(\nabla^2 - \lambda_2^2)\,\varphi_2 + \delta(x-\xi) = 0$ $\varphi_2 = (\nabla^2 - \lambda_1^2)\,(\nabla^2 - \lambda_3^2)\,(\nabla^2 - \lambda_4^2)\,\Phi$
$(\nabla^2 - \lambda_3^2)\,\varphi_3 + \delta(x-\xi) = 0$ $\varphi_3 = (\nabla^2 - \lambda_1^2)\,(\nabla^2 - \lambda_2^2)\,(\nabla^2 - \lambda_4^2)\,\Phi$	$(\nabla^2 - \lambda_4^2)\,\varphi_4 + \delta(x-\xi) = 0$ $\varphi_4 = (\nabla^2 - \lambda_1^2)\,(\nabla^2 - \lambda_2^2)\,(\nabla^2 - \lambda_3^2)\,\Phi$

2D Dynamic Fundamental Solutions for Unsat. Soils (cont.)

The solution in 2D:

$$\Phi = \frac{1}{2\pi}\left[\frac{K_0(\lambda_1 r)}{(\lambda_1^2-\lambda_3^2)(\lambda_1^2-\lambda_4^2)(\lambda_1^2-\lambda_2^2)} + \frac{K_0(\lambda_2 r)}{(\lambda_2^2-\lambda_4^2)(\lambda_2^2-\lambda_3^2)(\lambda_2^2-\lambda_1^2)} + \frac{K_0(\lambda_3 r)}{(\lambda_3^2-\lambda_2^2)(\lambda_3^2-\lambda_1^2)(\lambda_3^2-\lambda_4^2)} + \frac{K_0(\lambda_4 r)}{(\lambda_4^2-\lambda_1^2)(\lambda_4^2-\lambda_2^2)(\lambda_4^2-\lambda_3^2)}\right]$$

$r = |\mathbf{x} - \xi|$: Denotes the distance between a load point and an observation point.

$K_0(\lambda_k r)$: Denotes the modified Bessel function of the second kind of order zero.

2D Dynamic Fundamental Solutions for Unsat. Soils (cont.)

Last step is applying $\varphi(r,s)$ to $\mathbf{B}^{\star\, co}$:

$$\tilde{\mathbf{G}} = \begin{bmatrix} \tilde{G}_{\alpha\beta} & \tilde{G}_{\alpha w} & \tilde{G}_{\alpha a} \\ \tilde{G}_{w\beta} & \tilde{G}_{ww} & \tilde{G}_{wa} \\ \tilde{G}_{a\beta} & \tilde{G}_{aw} & \tilde{G}_{aa} \end{bmatrix} = \begin{bmatrix} \tilde{U}^{S}_{\alpha\beta} & \tilde{U}^{W}_{\alpha} & \tilde{U}^{A}_{\alpha} \\ \tilde{P}^{wS}_{\beta} & \tilde{P}^{wW} & \tilde{P}^{wA} \\ \tilde{P}^{aS}_{\beta} & \tilde{P}^{aW} & \tilde{P}^{aA} \end{bmatrix}$$

$$= \begin{bmatrix} B^{\star\, co}_{\alpha\beta} & B^{\star\, co}_{\alpha w} & B^{\star\, co}_{\alpha a} \\ B^{\star\, co}_{w\beta} & B^{\star\, co}_{ww} & B^{\star\, co}_{wa} \\ B^{\star\, co}_{a\beta} & B^{\star\, co}_{aw} & B^{\star\, co}_{aa} \end{bmatrix} \frac{\Phi}{\mu\,(\lambda+2\mu)\,k_w k_a}$$

$$B^{\star\, co}_{\alpha\beta} = \delta_{\alpha\beta}(\lambda+2\mu)k_w k_a(\nabla^2-\lambda_2^2)(\nabla^2-\lambda_3^2)(\nabla^2-\lambda_4^2) - \partial_\alpha\partial_\beta(C_1^{ss}\nabla^4 + C_2^{ss}s\nabla^2 + C_3^{ss}s^2)$$

$$B^{\star\, co}_{w\beta} = (C_1^{ws}\nabla^4 + C_2^{ws}s\nabla^2 + C_3^{ws}s^3)\partial_\beta \qquad B^{\star\, co}_{a\beta} = (C_1^{as}\nabla^4 + C_2^{as}s\nabla^2 + C_3^{as}s^3)\partial_\beta$$

$$B^{\star\, co}_{\alpha w} = (C_1^{sw}s\nabla^4 + C_2^{sw}s^2\nabla^2 + C_3^{sw}s^4)\partial_\alpha \qquad B^{\star\, co}_{\alpha a} = (C_1^{sa}s\nabla^4 + C_2^{sa}s^2\nabla^2 + C_3^{sa}s^4)\partial_\alpha$$

$$B^{\star\, co}_{wa} = (C_1^{wa}s\nabla^4 + C_2^{wa}s^3\nabla^2 - C_3^{wa}s^5) \qquad B^{\star\, co}_{aw} = (C_1^{aw}s\nabla^4 + C_2^{aw}s^3\nabla^2 + C_3^{aw}s^5)$$

$$B^{\star\, co}_{ww} = (C_1^{ww}\nabla^6 + C_2^{ww}s\nabla^4 + C_3^{ww}s^3\nabla^2 + C_4^{ww}s^5)$$

$$B^{\star\, co}_{aa} = (C_1^{aa}\nabla^6 + C_2^{aa}s\nabla^4 + C_3^{aa}s^3\nabla^2 + C_4^{aa}s^5)$$

2D Dynamic Fundamental Solutions for Unsat. Soils (cont.)

The final explicit forms of the fundamental solutions:

Displacement caused by a Dirac force in the solid:

$$\tilde{U}^{S}_{\alpha\beta} = \frac{1}{2\pi\mu}\left\{\begin{array}{l} \frac{-(\lambda+\mu)\Lambda^2}{\rho s^2}\frac{(\lambda_1^2-K_{ss1}^2)(\lambda_1^2-K_{ss2}^2)}{(\lambda_1^2-\lambda_2^2)(\lambda_1^2-\lambda_3^2)(\lambda_1^2-\lambda_4^2)}(R_1\lambda_1 K_1(\lambda_1 r)+R_2\lambda_1^2 K_0(\lambda_1 r))+ \\ \frac{-(\lambda+\mu)\Lambda^2}{\rho s^2}\frac{(\lambda_2^2-K_{ss1}^2)(\lambda_2^2-K_{ss2}^2)}{(\lambda_2^2-\lambda_1^2)(\lambda_2^2-\lambda_3^2)(\lambda_2^2-\lambda_4^2)}(R_1\lambda_2 K_1(\lambda_2 r)+R_2\lambda_2^2 K_0(\lambda_2 r))+ \\ \frac{-(\lambda+\mu)\Lambda^2}{\rho s^2}\frac{(\lambda_3^2-K_{ss1}^2)(\lambda_3^2-K_{ss2}^2)}{(\lambda_3^2-\lambda_1^2)(\lambda_3^2-\lambda_2^2)(\lambda_3^2-\lambda_4^2)}(R_1\lambda_3 K_1(\lambda_3 r)+R_2\lambda_3^2 K_0(\lambda_3 r))+ \\ \frac{-(\lambda+\mu)\Lambda^2}{\rho s^2}\frac{(\lambda_4^2-K_{ss1}^2)(\lambda_4^2-K_{ss2}^2)}{(\lambda_4^2-\lambda_1^2)(\lambda_4^2-\lambda_2^2)(\lambda_4^2-\lambda_3^2)}(R_1\lambda_4 K_1(\lambda_4 r)+R_2\lambda_4^2 K_0(\lambda_4 r)) \end{array}\right\} + \frac{\delta_{\alpha\beta}}{2\pi\mu}K_0(\lambda_1 r)$$

with $R_1 = (2r_{,\alpha}r_{,\beta} - \delta_{\alpha\beta}/r)$; $R_2 = r_{,\alpha}r_{,\beta}$

2D Dynamic Fundamental Solutions for Unsat. Soils (cont.)

The final explicit forms of the fundamental solutions:

Water pressure caused by a Dirac source in the water fluid:

$$\tilde{P}^{ww} = \frac{1}{2\pi k_w} \left\{ \begin{array}{l} \dfrac{1}{(\lambda_4^2-\lambda_2^2)(\lambda_3^2-\lambda_2^2)}(\lambda_2^2-K_w^2)(\lambda_2^2-\Lambda_w^2)K_0(\lambda_2 r)+ \\ \dfrac{1}{(\lambda_4^2-\lambda_3^2)(\lambda_2^2-\lambda_3^2)}(\lambda_3^2-K_w^2)(\lambda_3^2-\Lambda_w^2)K_0(\lambda_3 r)+ \\ \dfrac{1}{(\lambda_3^2-\lambda_4^2)(\lambda_2^2-\lambda_4^2)}(\lambda_4^2-K_w^2)(\lambda_4^2-\Lambda_w^2)K_0(\lambda_4 r) \end{array} \right\}$$

2D Dynamic Fundamental Solutions for Unsat. Soils (cont.)

The final explicit forms of the fundamental solutions:

Air pressure caused by a Dirac source in the air fluid:

$$\tilde{P}^{aA} = \frac{1}{2\pi k_a} \left\{ \begin{array}{l} \dfrac{1}{(\lambda_4^2-\lambda_2^2)(\lambda_3^2-\lambda_2^2)}(\lambda_2^2-K_a^2)(\lambda_2^2-\Lambda_a^2)K_0(\lambda_2 r)+ \\ \dfrac{1}{(\lambda_4^2-\lambda_3^2)(\lambda_2^2-\lambda_3^2)}(\lambda_3^2-K_a^2)(\lambda_3^2-\Lambda_a^2)K_0(\lambda_3 r)+ \\ \dfrac{1}{(\lambda_3^2-\lambda_4^2)(\lambda_2^2-\lambda_4^2)}(\lambda_4^2-K_a^2)(\lambda_4^2-\Lambda_a^2)K_0(\lambda_4 r) \end{array} \right\}$$

The other components of the fundamental solution matrix:

$$\rightsquigarrow \tilde{P}^{wS}_{\beta}, \tilde{P}^{aS}_{\beta}, \tilde{P}^{aW}, \tilde{P}^{wA}, \tilde{U}^{A}_{\alpha}, \tilde{U}^{W}_{\alpha}$$

Singular Behaviour

- In order to determine the unknown boundary data, it is necessary to know the behaviour of the fundamental solutions when $r = |\mathbf{x} - \xi|$ tends to zero, i.e. when an integration point $\mathbf{x}$ approaches a collocation point ξ.
- Simple series expansions of the fundamental solutions with respect to the variable $r = |\mathbf{x} - \xi|$ have to be done.
- As $r \rightarrow 0$, so does the argument of the modified Bessel functions:

$$K_0(\lambda_k r) = -\ln(\lambda_k r) + \mathcal{O}(r^2) = -\ln(\lambda_k) + \ln(1/r) + \mathcal{O}(r^2)$$

$$K_1(\lambda_k r) = \frac{1}{\lambda_k r} + \mathcal{O}(r^2)$$

Singular Behaviour

- After some algebraic manipulation

Components	Singularity	Equation
$\tilde{G}_{\alpha\beta} = \tilde{U}^{S}_{\alpha\beta}$	Weakly singular ($\ln r$)	$\frac{1}{8\pi}\frac{1}{\mu(1-\nu)}\left\{\frac{x_\alpha x_\beta}{r^2} - \delta_{\alpha\beta}\,(3-4\nu)\ln r\right\} + \mathcal{O}(r^0)$
$\tilde{G}_{\alpha w} = \tilde{U}^{W}_{\alpha}$	Weakly singular ($\ln r$)	$-\frac{r}{8\pi}\frac{(S_w-\rho_w k_w s)s}{(\lambda+2\mu)k_w}\,\frac{x_\alpha}{r}\,(1-2\ln r) + \mathcal{O}(r^0)$
$\tilde{G}_{\alpha a} = \tilde{U}^{A}_{\alpha}$	Weakly singular ($\ln r$)	$-\frac{r}{8\pi}\frac{(S_a-\rho_a k_a s)s}{(\lambda+2\mu)k_a}\,\frac{x_\alpha}{r}\,(1-2\ln r) + \mathcal{O}(r^0)$
$\tilde{G}_{w\beta} = \tilde{P}^{wS}_{\beta}$	Weakly singular ($\ln r$)	$\frac{r}{8\pi}\frac{F^s}{(\lambda+2\mu)k_w}\,\frac{x_\beta}{r}\,(1-2\ln r) + \mathcal{O}(r^0)$
$\tilde{G}_{a\beta} = \tilde{P}^{aS}_{\beta}$	Weakly singular ($\ln r$)	$\frac{r}{8\pi}\frac{(1-F^s)}{(\lambda+2\mu)k_a}\,\frac{x_\beta}{r}\,(1-2\ln r) + \mathcal{O}(r^0)$
$\tilde{G}_{ww} = \tilde{P}^{wW}$	Weakly singular ($\ln r$)	$-\frac{1}{2\pi k_w}\ln(r) + \mathcal{O}(r^0)$
$\tilde{G}_{aa} = \tilde{P}^{aA}$	Weakly singular ($\ln r$)	$-\frac{1}{2\pi k_a}\ln(r) + \mathcal{O}(r^0)$
$\tilde{G}_{aw} = \tilde{P}^{aW}$	Regular (1)	$\mathcal{O}(r^0)$
$\tilde{G}_{wa} = \tilde{P}^{wA}$	Regular (1)	$\mathcal{O}(r^0)$

Verification: elastodynamics fundamental solution

Letting k_w and k_a approach infinity and ρ_w, ρ_a and F^s equal zero, the roots of the determinant equation reduce to two and we will have:

$$\lambda_1^2 = \frac{\rho s^2}{\mu}, \quad \lambda_2^2 = \lambda_3^2 = 0, \quad \lambda_4^2 = \Lambda^2 = \frac{\rho s^2}{(\lambda + 2\mu)}$$

Then

$$\tilde{U}_\alpha^W = \tilde{U}_\alpha^A = 0 \qquad \tilde{P}_\beta^{wS} = \tilde{P}_\beta^{aS} = 0 \qquad \tilde{P}^{wW} = \tilde{P}^{aA} = 0 \qquad \tilde{P}^{aW} = \tilde{P}^{wA} = 0$$

$$\tilde{U}_{\alpha\beta}^S = \frac{1}{2\pi\rho C_2^2}\left(a\delta_{\alpha\beta} - b\frac{x_\alpha x_\beta}{r^2}\right)$$

in which

$$C_2^2 = \frac{\mu}{\rho}, \quad C_1^2 = \frac{(\lambda + 2\mu)}{\rho}$$

$$a = K_0\left(\frac{sr}{C_2}\right) + \frac{C_2}{sr}\left[K_1\left(\frac{sr}{C_2}\right) - \frac{C_2}{C_1}K_1\left(\frac{sr}{C_1}\right)\right]$$

$$b = K_2\left(\frac{sr}{C_2}\right) - \frac{C_2^2}{C_1^2}K_2\left(\frac{sr}{C_1}\right)$$

Visualization of Some Fundamental Solutions

An unsaturated soil with incompressible solid grains is considered in which the material properties were defined in the metric system as follows:

Mechanical parameters:

K_b $(-)$	E (N/m^2)	K_l $(-)$	a_e $(-)$	b_e $(-)$	e_0 $(-)$	σ_e $(-)$	n $(-)$	ρ_s (Kg/m^3)
3281	21×10^6	1678	2	0.2	0.4	35×10^5	0.4	2600

Water parameters:

ρ_w (Kg/m^3)	K_w (N/m^2)	a_w (m/s)	α_w $(-)$	S_{wu} $(-)$	β_w (Pa^{-1})	m_{suc} $(-)$	p_w (Pa)
1000	2.15×10^9	1.2×10^{-9}	5	0.05	1.08×10^{-8}	1	300×10^5

Air parameters:

ρ_a (Kg/m^3)	K_a (N/m^2)	b_a (m^2)	α_a $(-)$	μ_a $(N.s.m^{-2})$	P_{atm} (N/m^2)	p_a (Pa)
1	1.01×10^5	3×10^{-10}	4	1.846×10^{-5}	10^5	0

Visualization of Some Fundamental Solutions

$\tilde{U}^S_{11}$ displacement in direction 1 due to a unit point force in the same direction versus the distance r and the frequency ω.

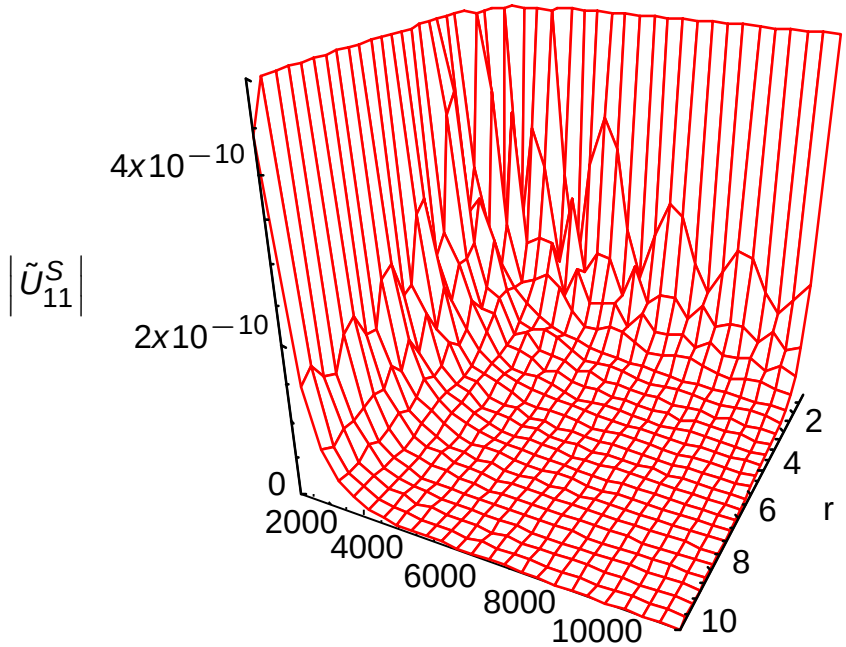

- The real part of the complex Laplace variable s is set to zero, i.e. $s = i\omega$
- The singular behaviour for small values of r is roughly independent of the frequency.
  Also, for a constant r away from the origin, a wave like form decrease of amplitudes is observed by increasing the frequencies.

Visualization of Some Fundamental Solutions

2D visualization by keeping constant the distance r and varying the frequency $s = i\omega$ to have a better insight into the behaviour of the fundamental solutions.

- The displacement and pressure results, are normalized to their singular behaviour.
- normalized displacement fundamental solution:

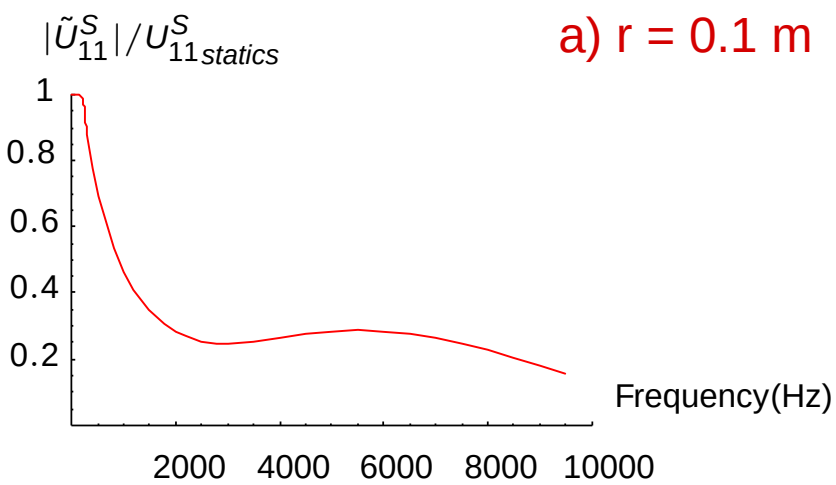

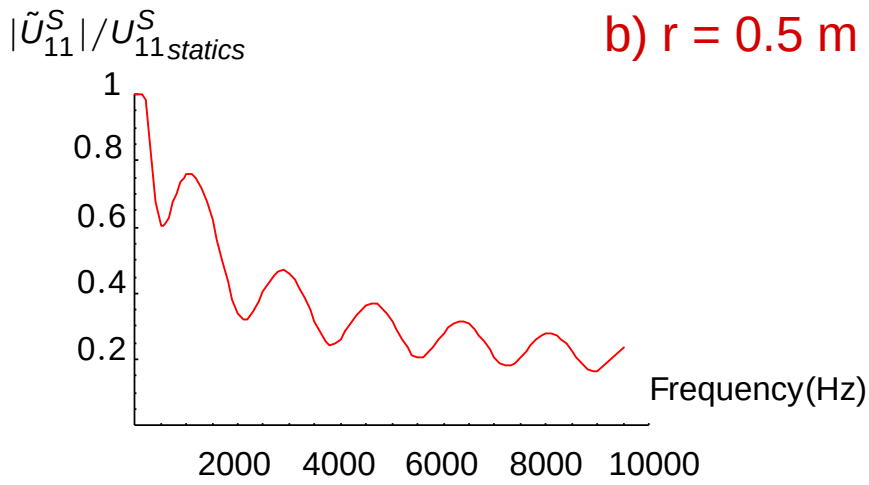

- There is a difference between the arrival times of the fast compressional wave. It is evident that the farther away the distance, the later the arrival time is, i.e., shorter frequency. Then in Fig. (b) at $0.5m$, the fast compressional wave arrives later and influences the shorter frequencies.

Visualization of Some Fundamental Solutions

Normalized water pressure fundamental solution due to a source in the water fluid:

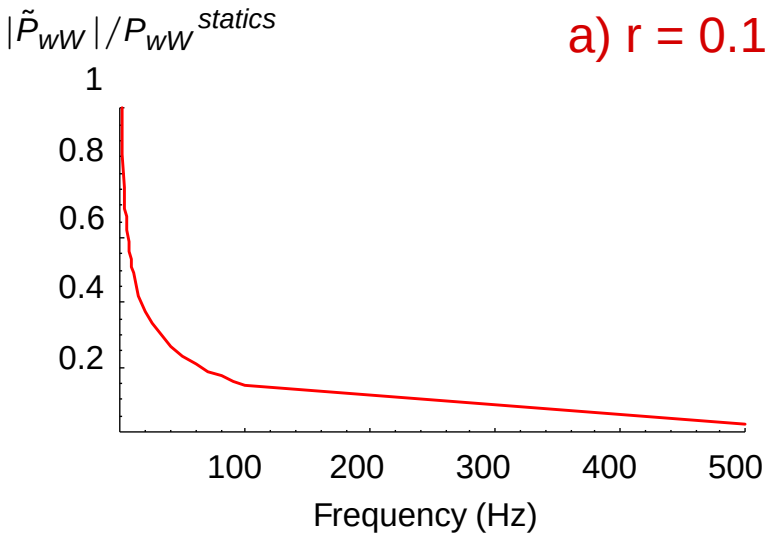

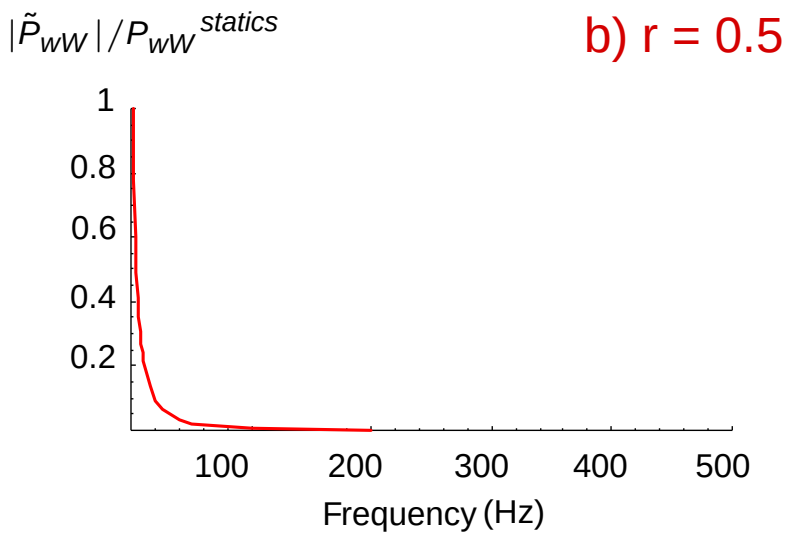

- A change in pressure is immediate in two cases. Therefore, the pressure cannot show a strong time, respectively frequency, dependence.

Boundary integral equation: Weighted residuals method

$$\int_\Omega \mathbf{B} \begin{bmatrix} \tilde{u}_\alpha \\ \tilde{p}_w \\ \tilde{p}_a \end{bmatrix} \tilde{\mathbf{G}}\, d\Omega = 0 \quad \text{avec} \quad \tilde{\mathbf{G}} = \begin{bmatrix} \tilde{G}_{\alpha\beta} & \tilde{G}_{\alpha w} & \tilde{G}_{\alpha a} \\ \tilde{G}_{w\beta} & \tilde{G}_{ww} & \tilde{G}_{wa} \\ \tilde{G}_{a\beta} & \tilde{G}_{aw} & \tilde{G}_{aa} \end{bmatrix} = \begin{bmatrix} \tilde{U}^S_{\alpha\beta} & \tilde{U}^W_\alpha & \tilde{U}^A_\alpha \\ \tilde{P}^{wS}_\beta & \tilde{P}^{wW} & \tilde{P}^{wA} \\ \tilde{P}^{aS}_\beta & \tilde{P}^{aW} & \tilde{P}^{aA} \end{bmatrix}$$

$\Rightarrow$ Two partial integrations $\Rightarrow$ Singular behavior $\Rightarrow$ Transformation to time domain

$$\begin{bmatrix} c_{\alpha\beta}(\xi) & 0 & 0 \\ 0 & c\,(\xi) & 0 \\ 0 & 0 & c\,(\xi) \end{bmatrix} \begin{bmatrix} u_\alpha(\xi;t) \\ p_w(\xi;t) \\ p_a(\xi;t) \end{bmatrix} =$$

$$\int_0^t \int_\Gamma \begin{bmatrix} U^S_{\alpha\beta}(x,\xi;t-\tau) & -P^{wS}_\alpha(x,\xi;t-\tau) & -P^{aS}_\alpha(x,\xi;t-\tau) \\ U^W_\beta(x,\xi;t-\tau) & -P^{wW}(x,\xi;t-\tau) & -P^{aW}(x,\xi;t-\tau) \\ U^A_\beta(x,\xi;t-\tau) & -P^{wA}(x,\xi;t-\tau) & -P^{aA}(x,\xi;t-\tau) \end{bmatrix} \begin{bmatrix} t_\alpha(x;\tau) \\ q_w(x;\tau) \\ q_a(x;\tau) \end{bmatrix} d\Gamma$$

$$- \int_0^t \oint_\Gamma \begin{bmatrix} T^S_{\alpha\beta}(x,\xi;t-\tau) & Q^{wS}_\alpha(x,\xi;t-\tau) & Q^{aS}_\alpha(x,\xi;t-\tau) \\ T^W_\beta(x,\xi;t-\tau) & Q^{wW}(x,\xi;t-\tau) & Q^{aW}(x,\xi;t-\tau) \\ T^A_\beta(x,\xi;t-\tau) & Q^{wA}(x,\xi;t-\tau) & Q^{aA}(x,\xi;t-\tau) \end{bmatrix} \begin{bmatrix} u_\alpha(x;\tau) \\ p_w(x;\tau) \\ p_a(x;\tau) \end{bmatrix} d\Gamma$$

Discretization in time: Convolution Quadrature Method (CQM) [1]

Quadrature rule for $n = 0, 1, \ldots, N$ time steps:

$$y(t) = f(t) * g(t) = \int_0^t f(t-\tau) g(\tau) d\tau \quad \Rightarrow \quad y(n\Delta t) = \sum_{k=0}^{n} \omega_{n-k}(\tilde{f}, \Delta t) g(k\Delta t)$$

Integration weight:

$$\omega_n(\Delta t) = \frac{1}{2\pi i} \int_{|z|=R} \tilde{f}\left(\frac{\gamma(z)}{\Delta t}\right) z^{-n-1} dz \approx \frac{R^{-n}}{L} \sum_{l=0}^{L-1} \underbrace{\tilde{f}\left(\frac{\gamma\left(Re^{il\frac{2\pi}{L}}\right)}{\Delta t}\right)}_{S_l} e^{-inl\frac{2\pi}{L}}$$

- $\gamma(z)$ A-stable multi step method, e.g. BDF 2: $\gamma(z) = 3/2 - 2z + z^2/2$
- Δt time step size of equal duration
- $L = N$ effective choice for determining ω_n (FFT)
- $R^N = \sqrt{\varepsilon}$ with $\varepsilon = 10^{-10}$

[1] Lubich C. (1988). I, II. Numerische Mathematik, Vol. 52

Discretizations in time and in space

Temporal discretization with CQM yields for $n = 1, 2, \ldots, N$:

$$c_{ij}(\xi)u_j^N(\xi) = \sum_{n=1}^{N}\left(\int_\Gamma (\omega_{ij}^G)^{N-n+1}(\mathbf{x},\xi)t_j^n(\mathbf{x})d\Gamma - \int_\Gamma (\omega_{ij}^H)^{N-n+1}(\mathbf{x},\xi)u_j^n(\mathbf{x})d\Gamma\right)$$

in which

$$(\omega_{ij}^G)^m(\mathbf{x},\xi) = \frac{R^{-m}}{L}\sum_{l=0}^{L-1}\tilde{G}_{ij}(\mathbf{x},\xi;s_l)e^{-iml\frac{2\pi}{L}} \quad ; \quad (\omega_{ij}^H)^m(\mathbf{x},\xi) = \frac{R^{-m}}{L}\sum_{l=0}^{L-1}\tilde{H}_{ij}(\mathbf{x},\xi;s_l)e^{-iml\frac{2\pi}{L}}$$

Spatial discretization:

$$c_{ij}U_j^N(\xi) = \sum_{n=1}^{N}\sum_{e=1}^{E}\sum_{m=1}^{M=3}\left[\left(T_{jm}^e\right)^n\left(\Delta G_{ij\,m}^e\right)^{N-n+1} - \left(U_{jm}^e\right)^n\left(\Delta H_{ij\,m}^e\right)^{N-n+1}\right]$$

in which

$$\left(\Delta G_{ij\,m}^e\right)^{N-n+1} = \int_{-1}^{1}\left(\omega_{ij}^G\right)^{N-n+1}(\mathbf{x}(\eta),\xi)N_m(\eta)|J(\eta)|d\eta$$
$$\left(\Delta H_{ij\,m}^e\right)^{N-n+1} = \int_{-1}^{1}\left(\omega_{ij}^H\right)^{N-n+1}(\mathbf{x}(\eta),\xi)N_m(\eta)|J(\eta)|d\eta$$

1 Unsaturated soils
- General context and fields of application
- Basic assumptions
- Governing equations

2 Boundary element method
- Problematics
- Fundamental Solution
- Boundary Integral Equation
- Discretization

3 Implementation in « HYBRID » FEM/BEM code
- Programming
- Validation

4 Applications in seismic site effects
- Introduction
- Topographic site effects in 2D configurations
- Combined effects in fully-filled alluvial valleys
- Alluvial effect in a partially-filled valley

5 Conclusion and Perspective

Characteristics

HYBRID code by Gatmiri and his colleagues (1997-2005).

Near field: Finite Element Method

- Dry and saturated soils
- Isotropic and anisotropic linear elastic behaviour (Gatmiri, Géotechnique 1990 and Gatmiri, ASCI 1992)
- Non-linear elastic behaviour (Gatmiri & Kamalian NUMOG VI 1999)
- Static, consolidation and dynamic problems for bounded domain

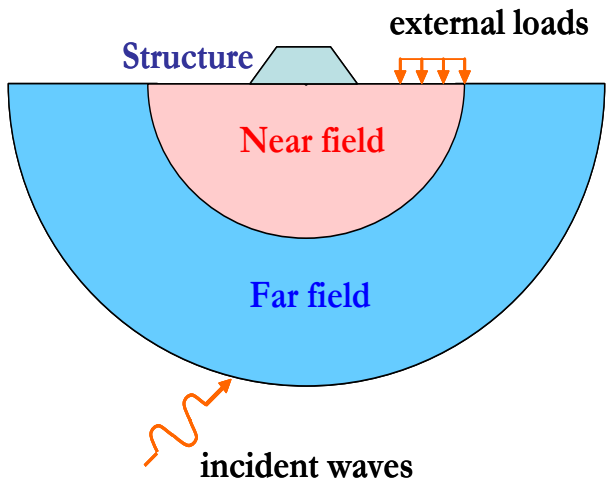

Characteristics

Far field: Boundary Element Method

- Dry and saturated soils
- Isotropic linear elastic behaviour
- Dynamics problems for bounded (D1), infinite (D2) and semi-infinite (D3) domains

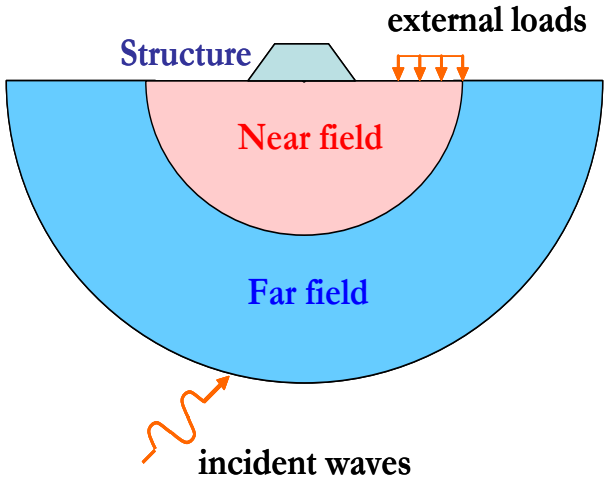

Characteristics

Application

Numerical tool for

- ISS modeling
- Simulation, validation and identification of seismic hazards:
  - *Seismic site effects (effects of topography and geology on the seismic response of sedimentary valleys)*

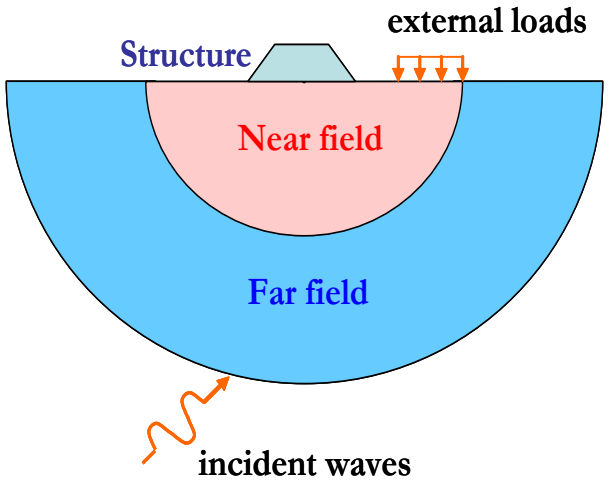

BEM part

BEM part of HYBRID code before 2007	
Elastodynamic	Linear elasticity (Gatmiri & Kamalian 1999, Gatmiri & Kamalian 2002) for bounded (D1), infinite (D2) and semi-infinite (D3) domains
Saturated poroelastodynamic	Linear elasticity (Gatmiri & Nguyen 2005, Nguyen & Gatmiri 2007, Gatmiri et al. 2008) using usual time-stepping method based on the fundamental solutions obtained in time domain (Gatmiri & Nguyen 2005) by considering the simplifying assumption of incompressible constituents
Developments done during this research	
Saturated soils	Consolidation problem: using CQM, based on the fundamental solutions obtained by Cheng & Detournay (1988) Wave propagation problem: using CQM, based on the fundamental solutions obtained by Schanz & Pryl (2004)
Unsaturated soils	Consolidation problem: using CQM, based on the fundamental solutions obtained by Maghoul et al. BeTeq (2010) Wave propagation problem Maghoul et al. JMM (2010): using CQM, based on the fundamental solutions obtained by Maghoul et al. SDEE (2010)

Consolidation problem in saturated soils

- The displacement response and the pore pressure distribution of a 2-d bar are compared with the analytical result presented by Detournay & Cheng (1993).
- The displacement response and the pore pressure distribution of a 2-d bar is compared with a Finite Element (FEM) calculation (the FEM code DIANA-SWANDYNE II)

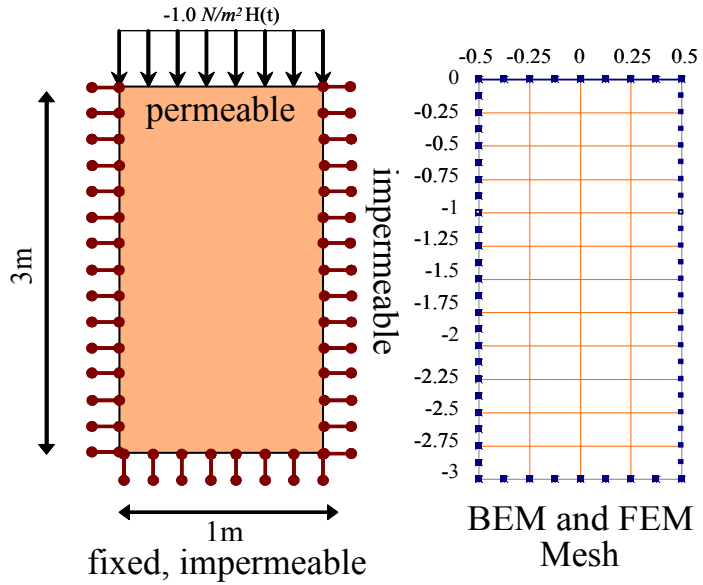

Material data of a soil (coarse sand):

$G(N/m^2)$	$\nu(-)$	$n(-)$	$\alpha(-)$	$\nu_u(-)$	$\kappa(m^4/N.s)$
9.8×10^7	0.298	0.48	0.980918	0.49	3.55×10^{-9}

Consolidation problem in saturated soils

Boundary conditions

- The bar is fixed at one end and loaded with $t_y = 1N/m^2 H(t)$ over the whole time period on the other end.
- At the other surfaces the normal displacements are blocked and in tangential directions free sliding, i.e., zero traction, is modeled.
- The free surface where the load as total stress function is applied is assumed to be permeable, i.e., the prescribed pore pressure vanishes.
- All other surfaces including the fixed end are impermeable, i.e., the flux vanishes there.

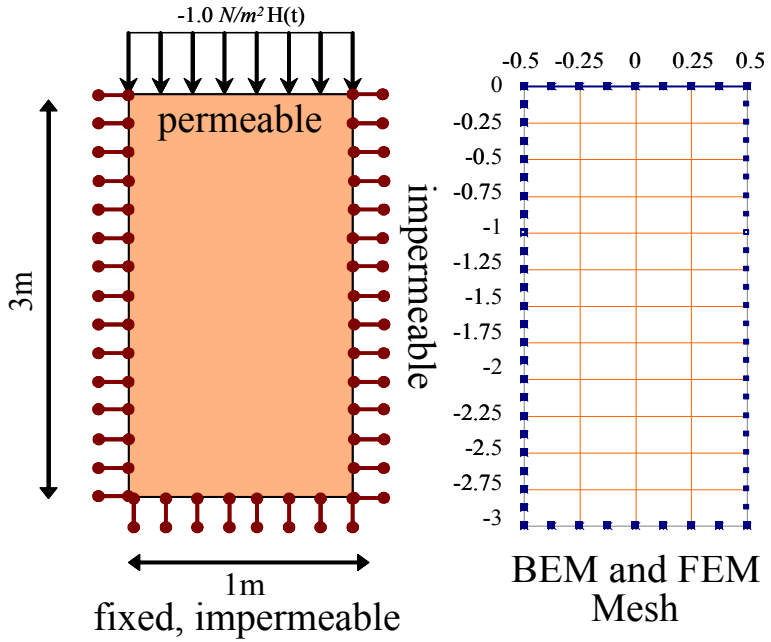

Consolidation problem in saturated soils

Displacement at the free end of the bar versus time: BEM results compared with FEM results and the analytical solution (logscale in time)

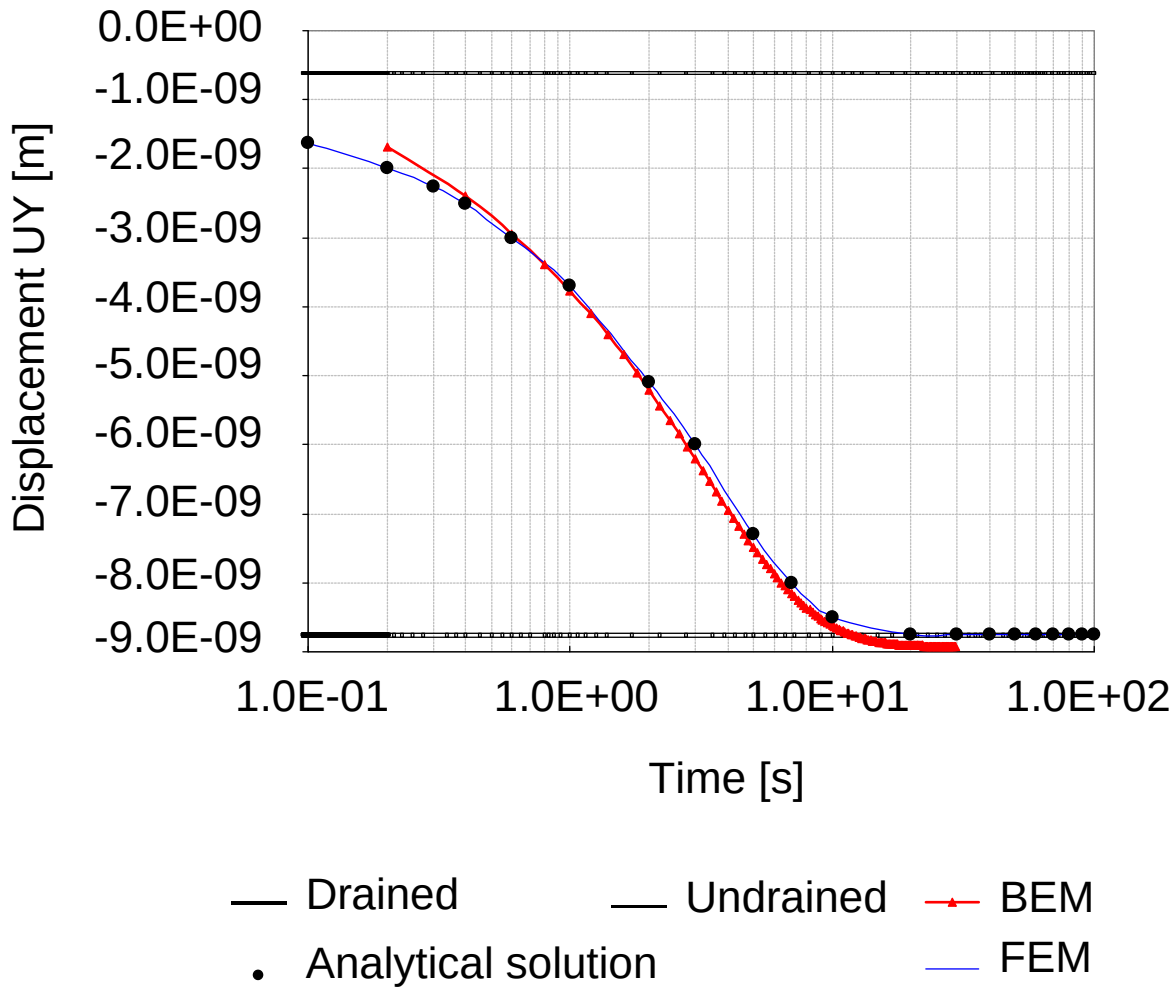

Consolidation problem in saturated soils

Pressure distribution along the mid-line of the bar: BEM results compared with FEM results and the analytical solution for different times

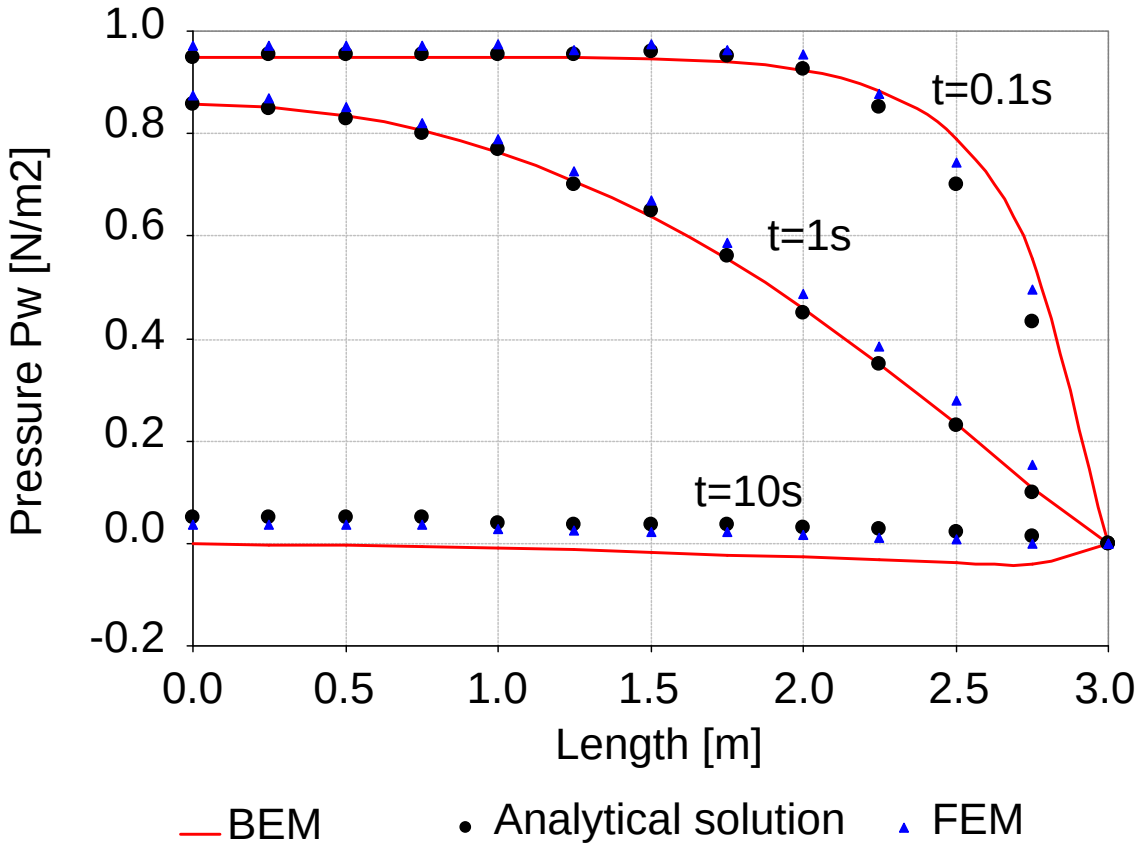

Wave propagation problem in saturated soils

- The displacement response and the pore pressure distribution of a 2-d bar are compared with the analytical result presented by Schanz & Struckmeier (2005).

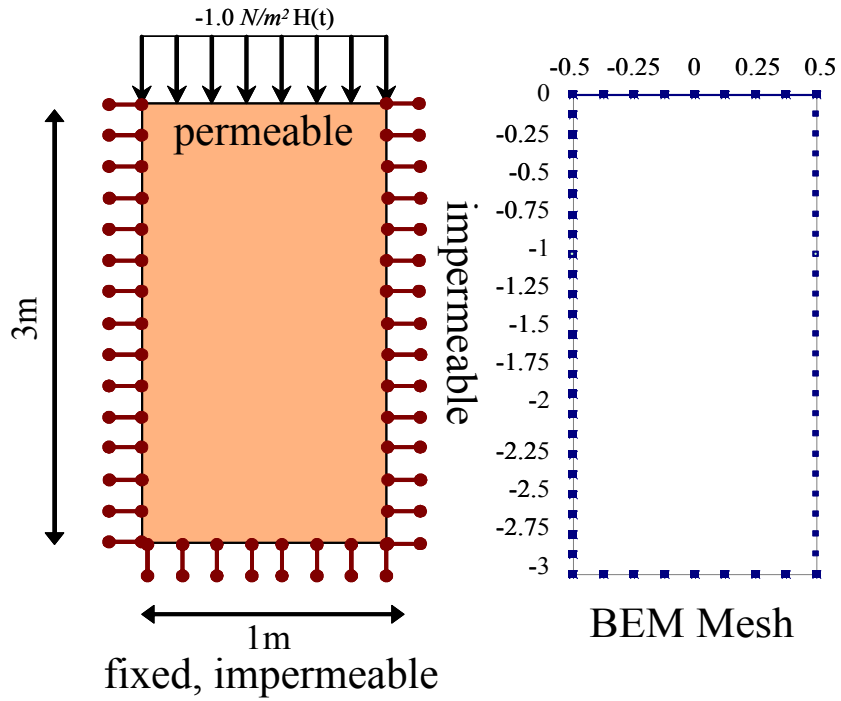

Material data of Berea sandstone (rock) and water saturated soil:

$E(N/m^2)$	$\nu(-)$	$n(-)$	$\alpha(-)$	$R(N/m^2)$	$\kappa(m^4/N.s)$	$\rho(kg/m^3)$	$\rho_f(kg/m^3)$
1.44×10^{10}	0	0.19	0.86	4.7×10^8	1.9×10^{-10}	2458	1000

Wave propagation problem in saturated soils

Boundary conditions

- The bar is fixed at one end and loaded with $t_y = 1N/m^2 H(t)$ over the whole time period on the other end.
- At the other surfaces the normal displacements are blocked and in tangential directions free sliding, i.e., zero traction, is modeled.
- The free surface where the load as total stress function is applied is assumed to be permeable, i.e., the prescribed pore pressure vanishes.
- All other surfaces including the fixed end are impermeable, i.e., the flux vanishes there.

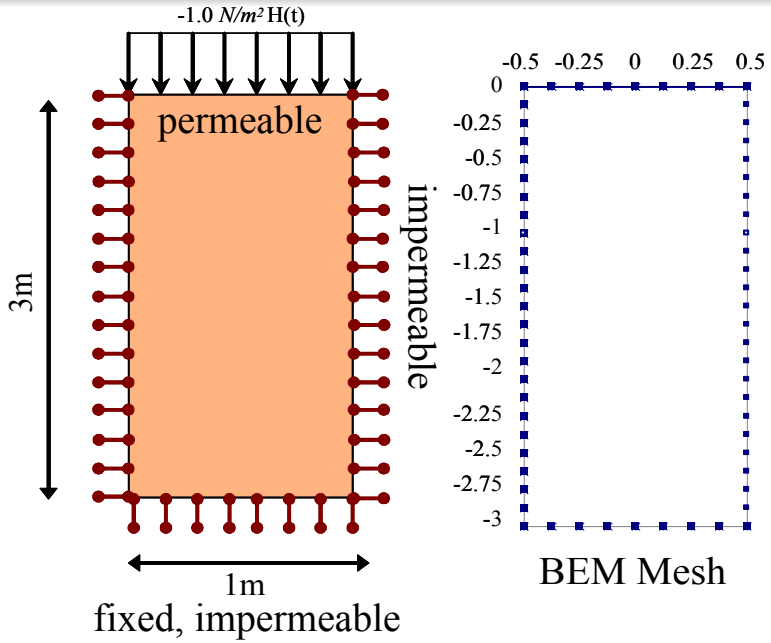

Wave propagation problem in saturated soils

Displacement in y-direction at the top of the column versus time: BEM results compared with the analytical solution.

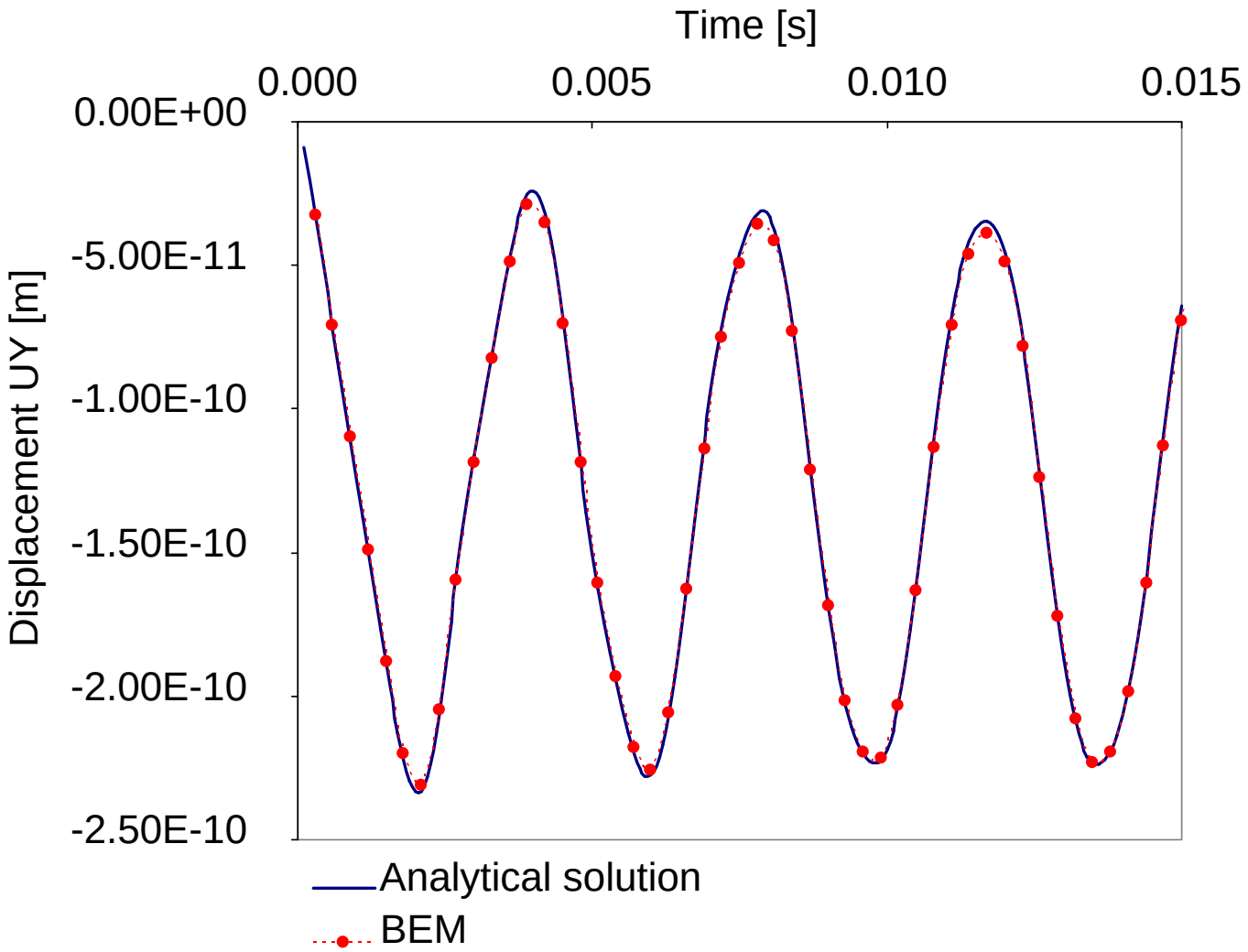

Wave propagation problem in saturated soils

Pressure at the bottom of the column versus time: BEM results compared with the analytical solution

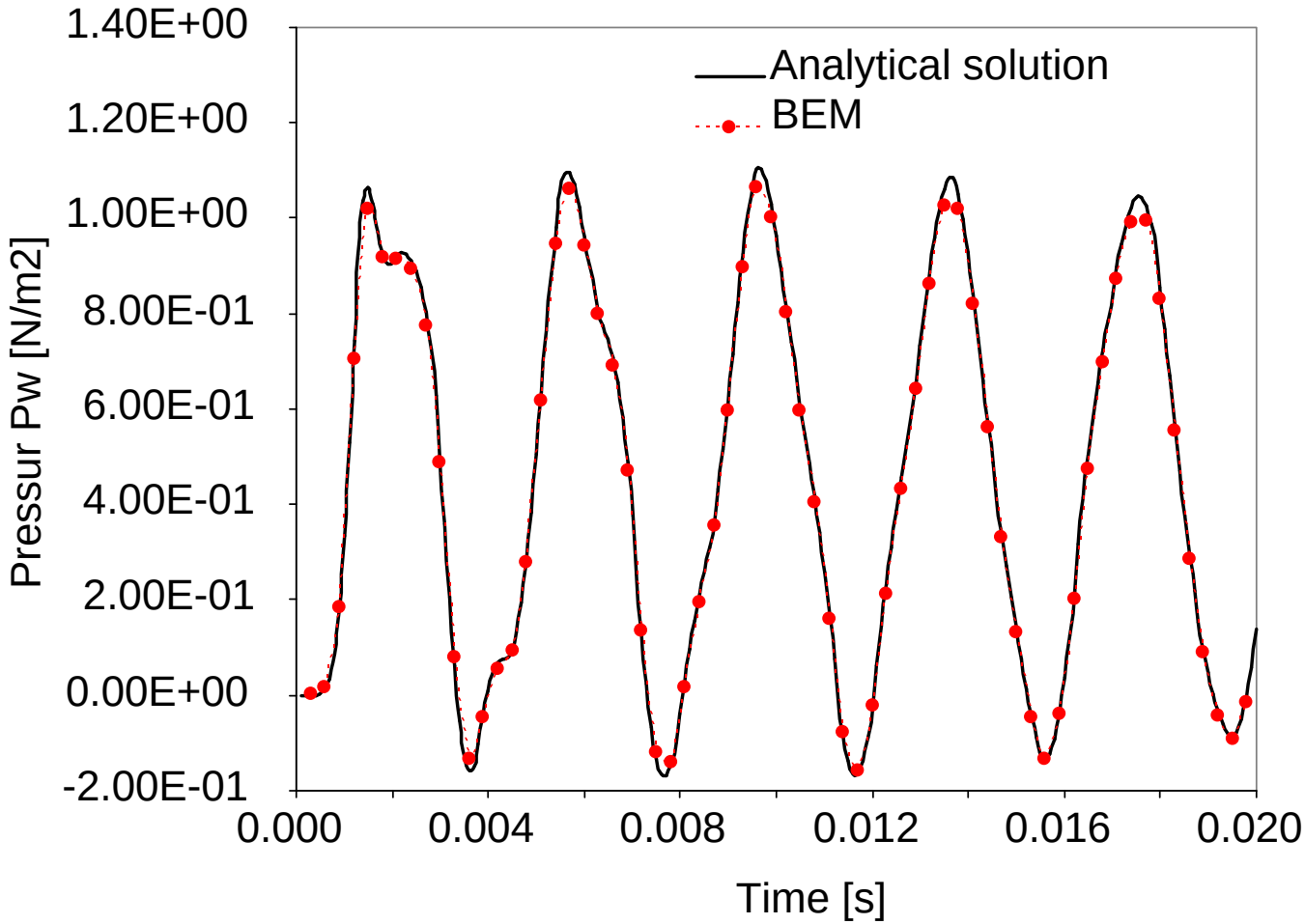

Unsaturated soils: Comparison with elastostatic problem

No analytical solution!

Boundary conditions

- The bar is fixed at one end and loaded with $t_y = 1000 N/m^2 H(t)$ over the whole time period on the other end.
- At the bottom end the normal and the tangential displacements are blocked.
- At the lateral surfaces the normal displacements are blocked and in tangential directions free sliding, i.e., zero traction, is modeled.
- The free surface where the load as total stress function is applied and all other surfaces including the fixed end are assumed to be permeable, i.e., the prescribed water pore pressure vanishes.
- The prescribed air pore pressure in all surfaces are assumed to be zero.

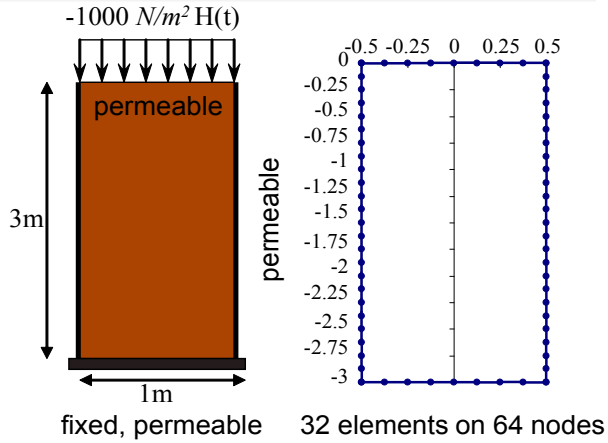

Unsaturated soils: Comparison with elastostatic problem

No analytical solution!

Material data of an unsaturated soil:

$E(N/m^2)$	$K_0(N/m^2)$	$a_e(-)$	$b_e(-)$	$e_0(-)$	$\sigma_e(N/m^2)$
2.54×10^{10}	2.1×10^{10}	1.0	0.15	0.73	8.5×10^{8}
$a_w(m/s)$	$\alpha_w(-)$	$S_{ru}(-)$	$b_a(m^2)$	$\mu_a(Ns/m^2)$	$a_s(m^2/N)$
1.2×10^{-8}	5.0	0.05	1.0×10^{-8}	1.846×10^{-5}	-5.0×10^{-7}

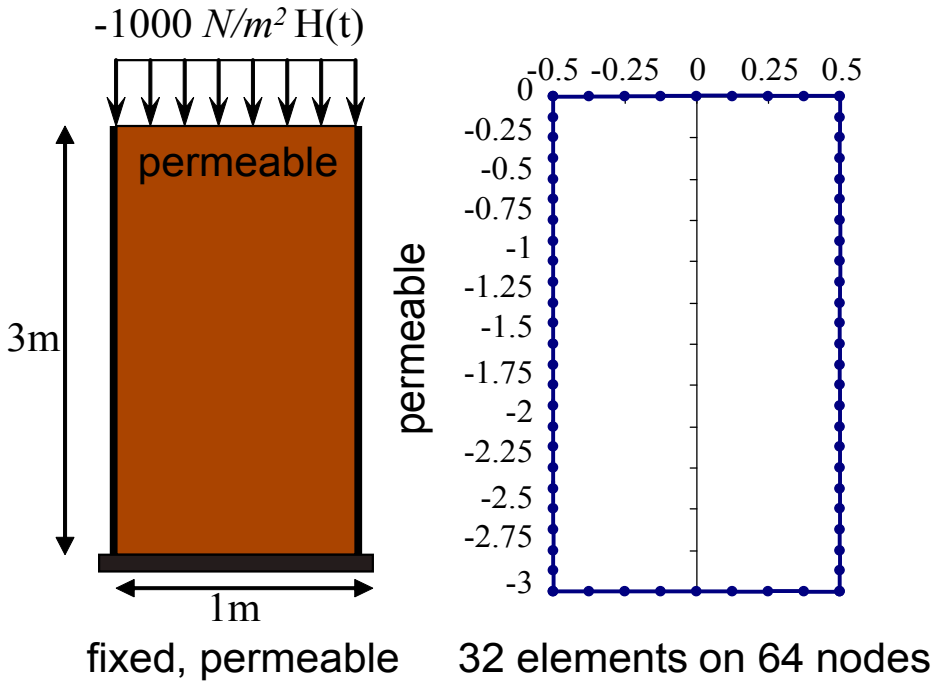

fixed, permeable

32 elements on 64 nodes

Unsaturated soils: Comparison with elastostatic problem

The absolute values of vertical displacements along the midline of the column:

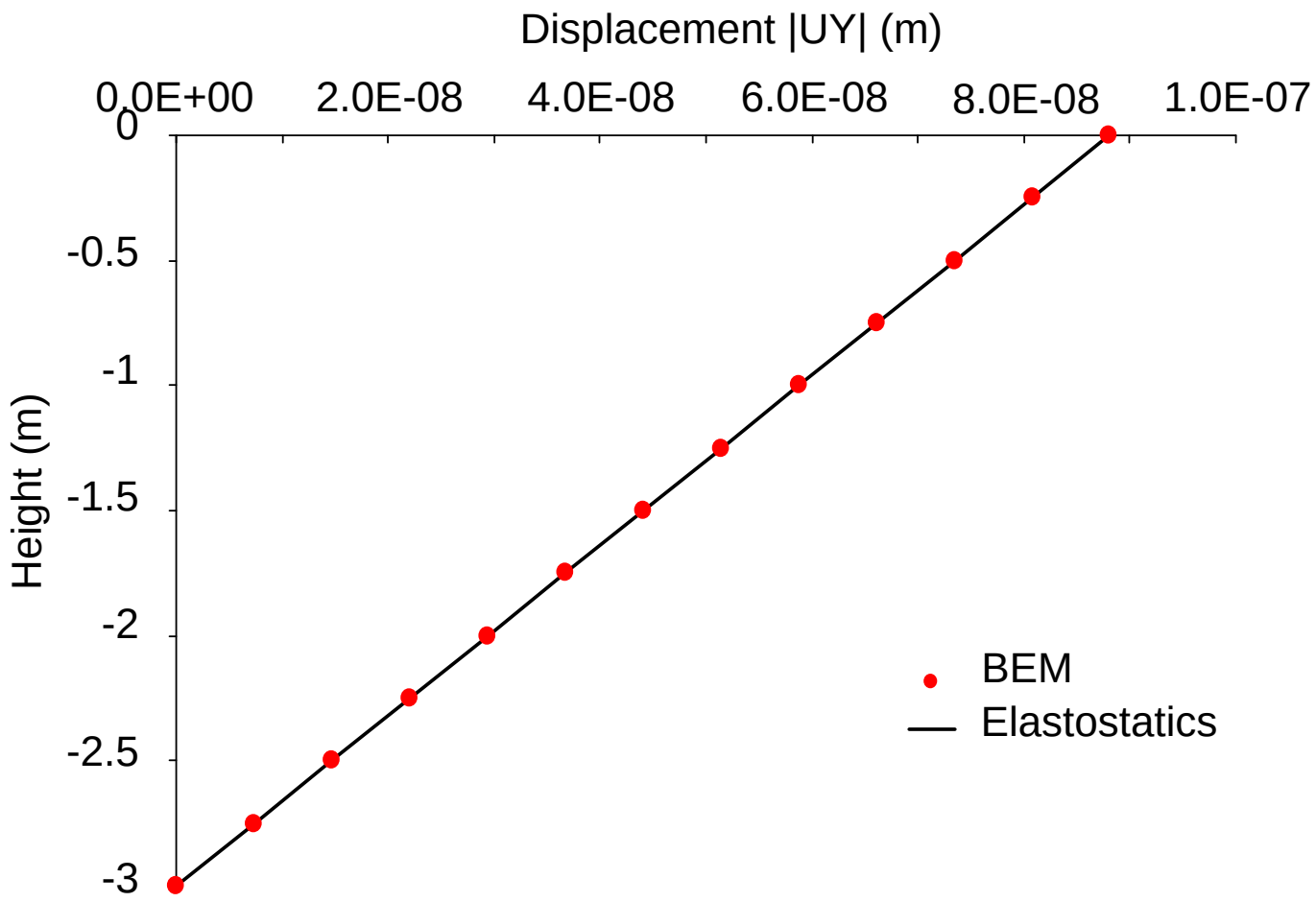

Unsaturated soils: Comparison with elastodynamics problem

No analytical solution!

Boundary conditions

- The bar is fixed at one end and loaded with $t_y = 1000N/m^2 H(t)$ over the whole time period on the other end.
- At the bottom end the normal and the tangential displacements are blocked.
- At the lateral surfaces the normal displacements are blocked and in tangential directions free sliding, i.e., zero traction, is modeled.
- The free surface where the load as total stress function is applied and all other surfaces including the fixed end are assumed to be permeable, i.e., the prescribed water pore pressure vanishes.
- The prescribed air pore pressure in all surfaces are assumed to be zero.

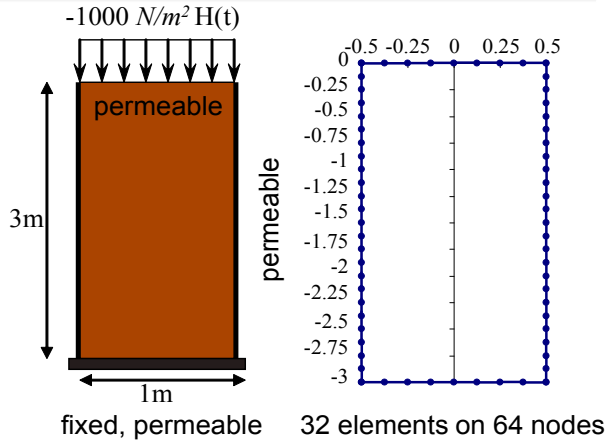

Unsaturated soils: Comparison with elastodynamics problem

No analytical solution!

Material data of an unsaturated soil:

$E(N/m^2)$	$K_0(N/m^2)$	$a_e(-)$	$b_e(-)$	$e_0(-)$	$\sigma_e(N/m^2)$
2.54×10^{10}	2.1×10^{10}	1.0	0.15	0.73	8.5×10^{8}
$a_w(m/s)$	$\alpha_w(-)$	$S_{ru}(-)$	$b_a(m^2)$	$\mu_a(Ns/m^2)$	$a_s(m^2/N)$
1.2×10^{-8}	5.0	0.05	1.0×10^{-8}	1.846×10^{-5}	-5.0×10^{-7}

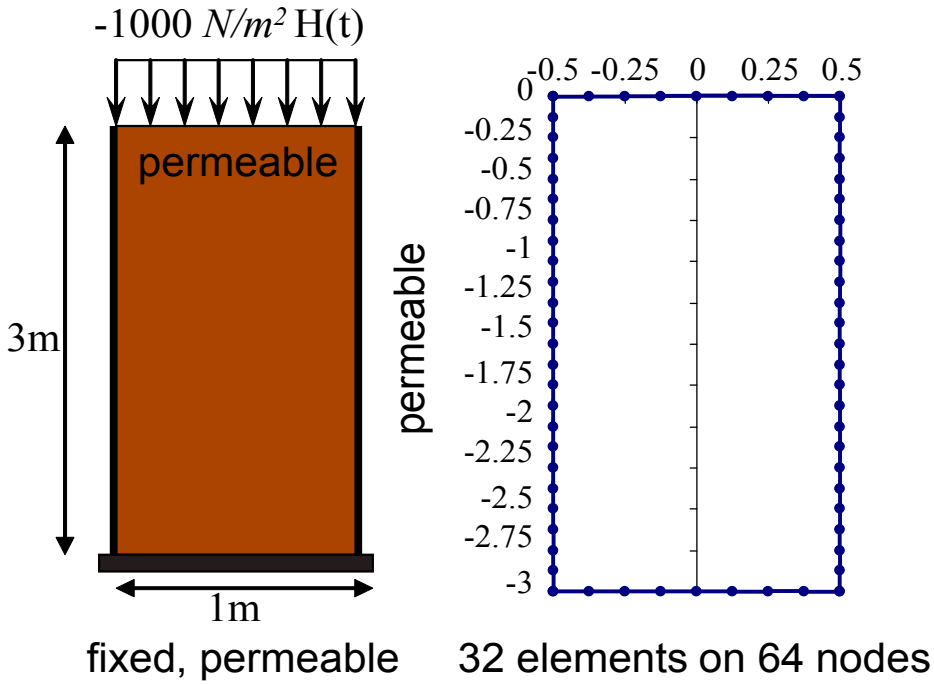

Unsaturated soils: Comparison with elastodynamics problem

Vertical displacements obtained for the midpoint of the upper surface of the column:

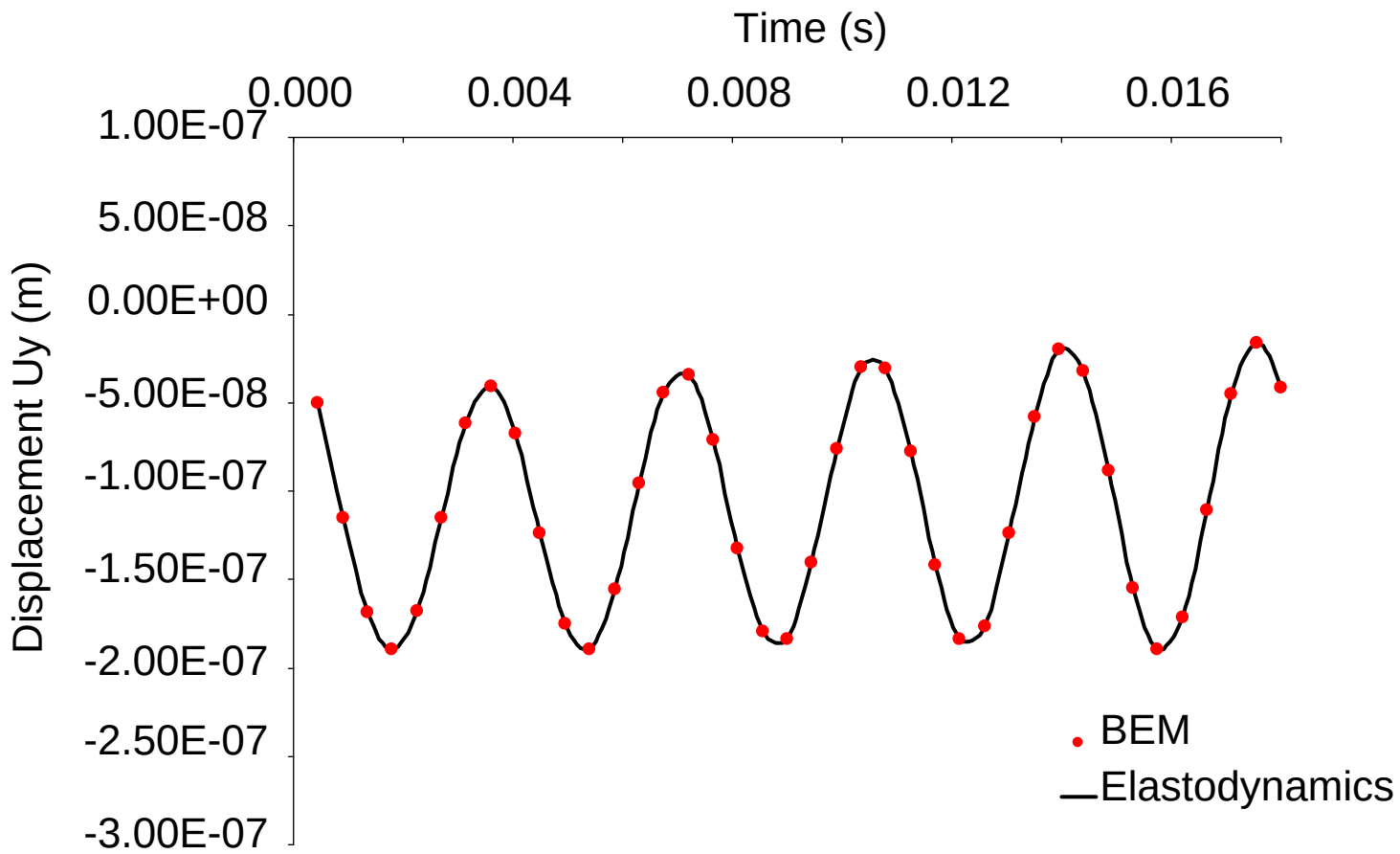

1 Unsaturated soils
- General context and fields of application
- Basic assumptions
- Governing equations

2 Boundary element method
- Problematics
- Fundamental Solution
- Boundary Integral Equation
- Discretization

3 Implementation in « HYBRID » FEM/BEM code
- Programming
- Validation

4 **Applications in seismic site effects**
- Introduction
- Topographic site effects in 2D configurations
- Combined effects in fully-filled alluvial valleys
- Alluvial effect in a partially-filled valley

5 Conclusion and Perspective

Site effect

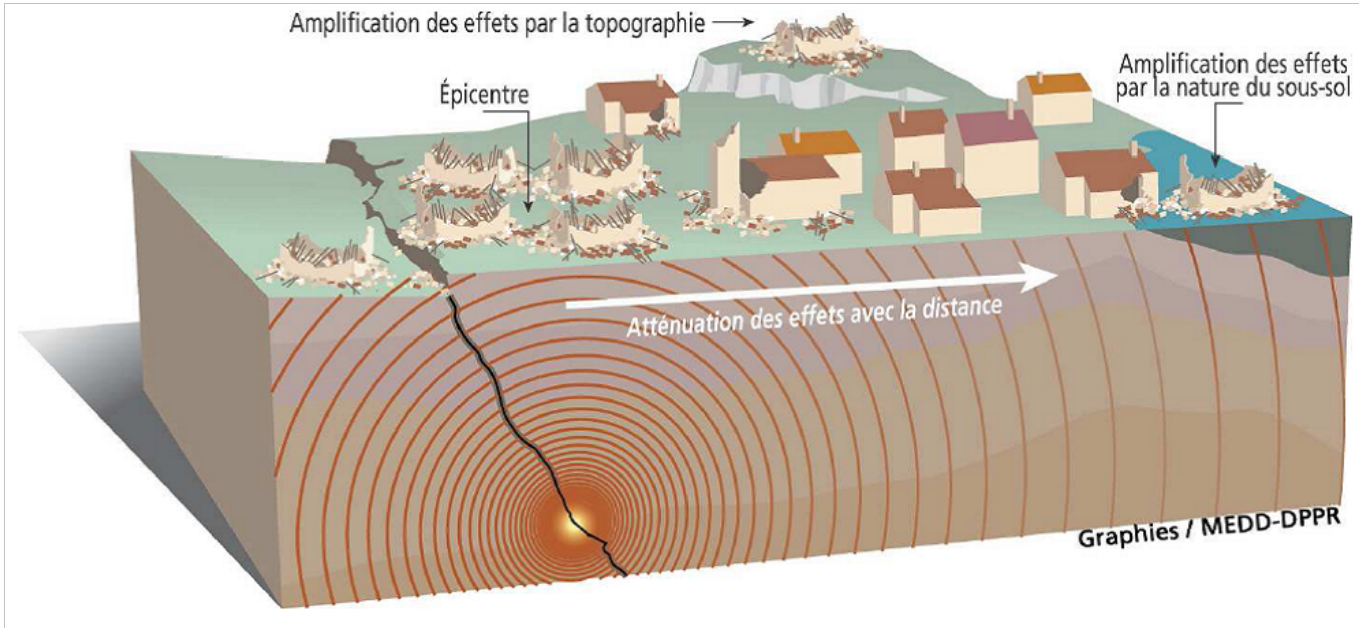

- It has been often observed, after earthquakes, that some buildings located on hills or in sedimentary basins suffer important damage with regard to their distance to the epicentre.
- The modification of the seismic movement due to local topographical and geotechnical conditions is called **site effect**.

Seismic codes and one-dimensional (1D) model

- The majority of actual seismic codes rest on the sedimentary effects by using a one-dimensional (1D) model.
- This method allows us to measure the influence of nature and thickness of the sedimentary layer on the vertical propagation of the volumic waves.
- These results do not agree with estimates provided by two-dimensional or three-dimensional models.

$$\Downarrow$$

It is necessary to take into account the influence of topographical and geological conditions on seismic movement in normal engineering practice.

Objectives

- Study the combined effect of:
  - Geometrical characteristics
  - Impedance contrast between sediments and bedrock

$$\beta = \frac{\rho_s V_s}{\rho_r V_r}$$

ρ_s: Soil density (kg/m^3)

V_s: Shear wave velocity in sediments (m/s)

ρ_r: Bedrock density (kg/m^3)

V_r: Shear wave velocity in bedrock (m/s)

- Define simple criteria combining soil properties and geometrical characteristics of the valley
- Predict the amplification of the earthquake response spectrum in alluvial and empty valleys

Parameters of the problem

Geometrical characteristics: Configurations of the studied valleys are triangle, trapezium, rectangle, ellipse and truncated ellipse.

$L = 100$ $L_1/L = 0, 0.4$ $H/L = 0.2, 0.4, 0.6, 1$

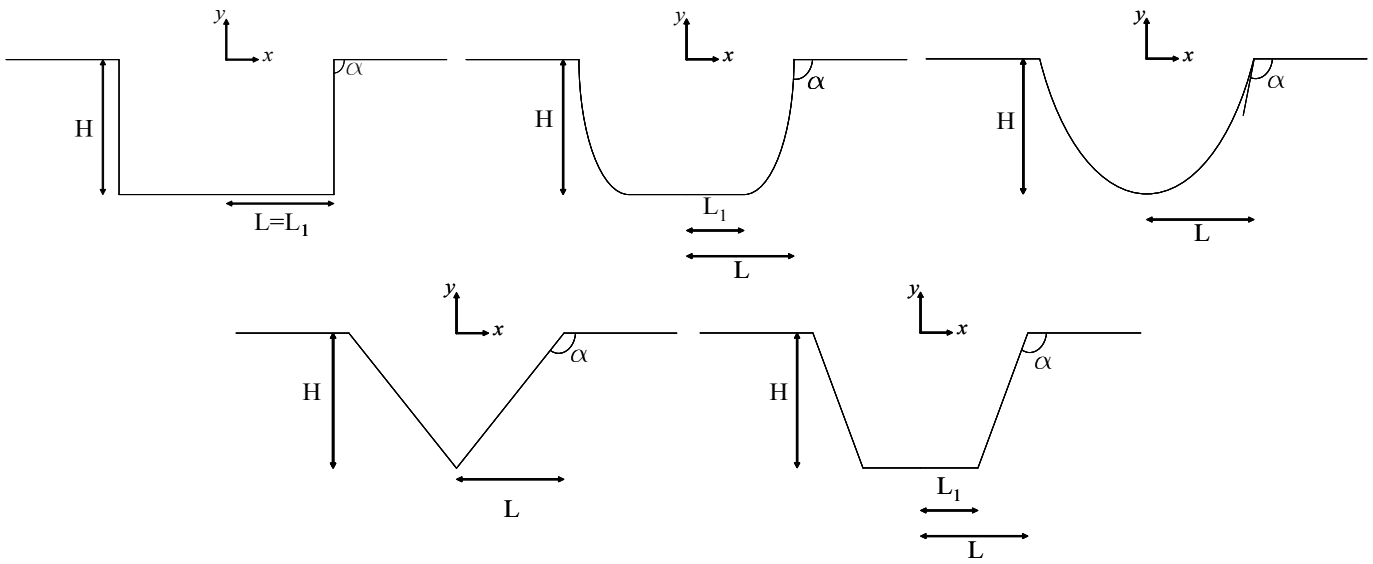

Soil properties:

	E (MPa)	K (MPa)	ν (-)	G (MPa)	ρ (Kg/m^3)	v_S (m/s)	Impedance (α) (-)
Bedrock	6720.0	11200.0	0.4	24.0	2.45×10^3	1000.0	1.0

Seismic solicitation: Vertically incident SV Ricker wave with predominant frequency of 2Hz.

Study of the topographical effects in the various empty valleys

- Some geometrical points are chosen as stations
- A triplet of curves is obtained for every chosen observation point and for every type of valley (acceleration response spectrum for each observation point, acceleration response spectrum for the reference site and spectral ratio)

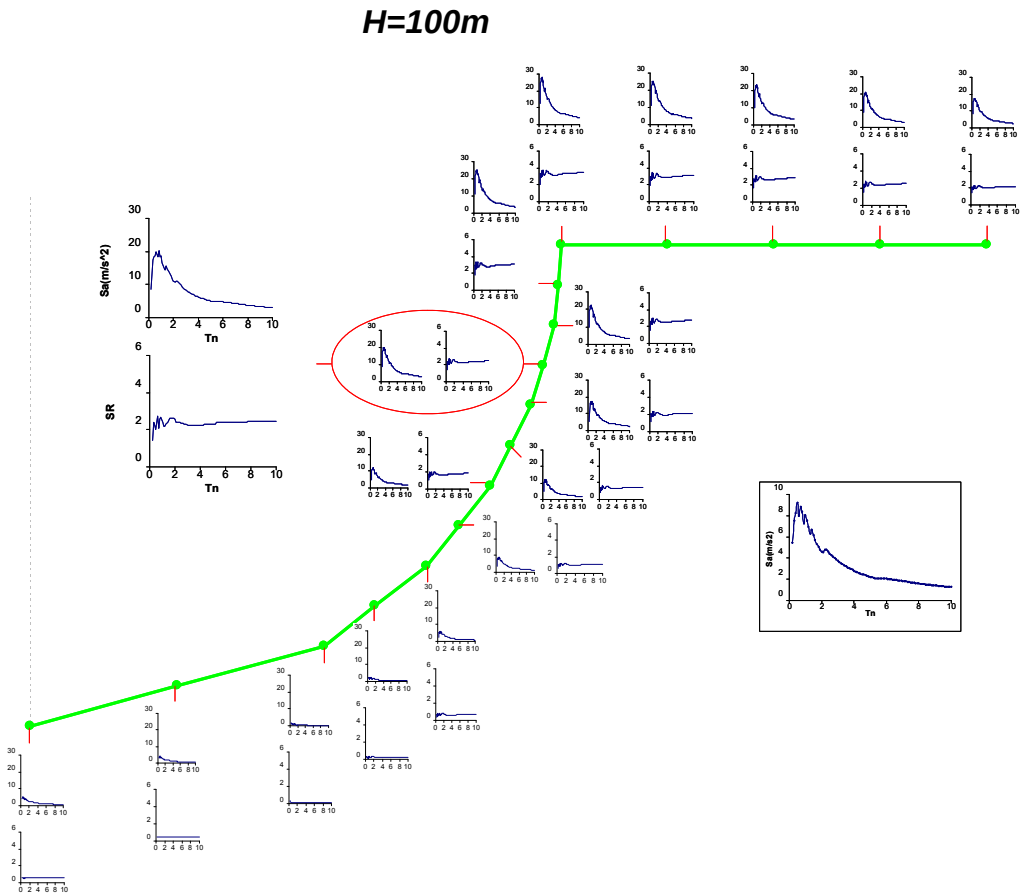

Study of the topographical effects in the various empty valleys

- Some geometrical points are chosen as stations
- A triplet of curves is obtained for every chosen observation point and for every type of valley (acceleration response spectrum for each observation point, acceleration response spectrum for the reference site and spectral ratio)

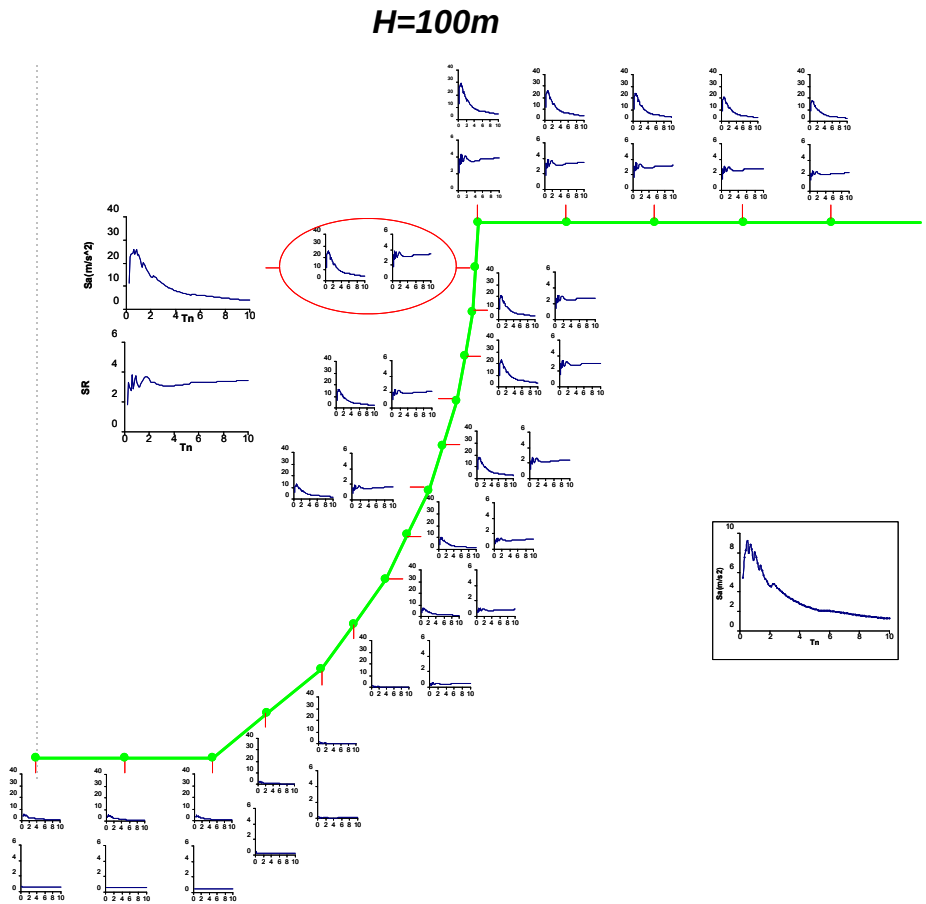

Study of the topographical effects in the various empty valleys

- Some geometrical points are chosen as stations
- A triplet of curves is obtained for every chosen observation point and for every type of valley (acceleration response spectrum for each observation point, acceleration response spectrum for the reference site and spectral ratio)

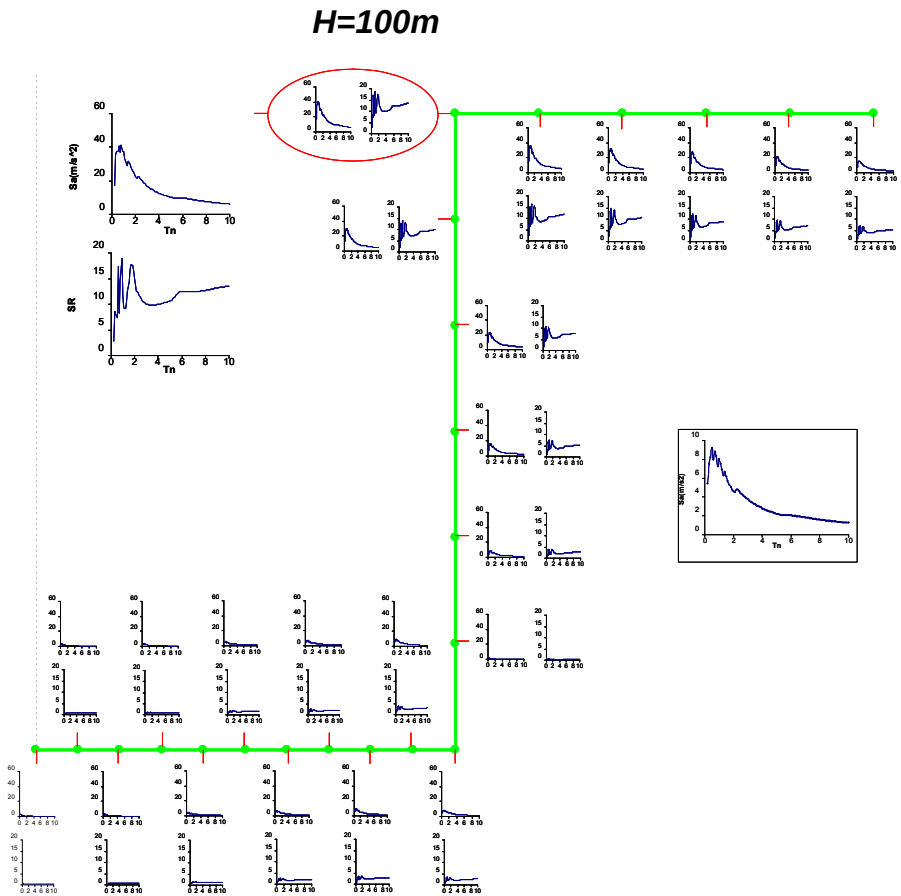

Study of the topographical effects in the various empty valleys

- Some geometrical points are chosen as stations
- A triplet of curves is obtained for every chosen observation point and for every type of valley (acceleration response spectrum for each observation point, acceleration response spectrum for the reference site and spectral ratio)

H=100m

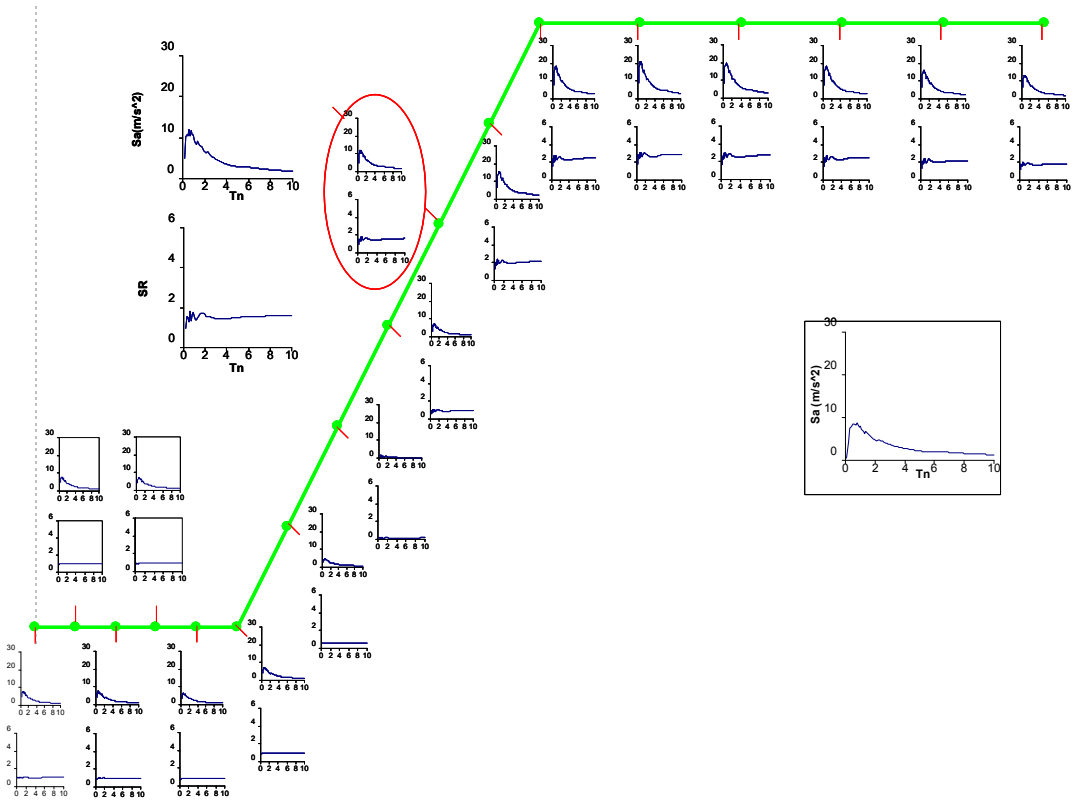

Study of the topographical effects in the various empty valleys

- Some geometrical points are chosen as stations
- A triplet of curves is obtained for every chosen observation point and for every type of valley (acceleration response spectrum for each observation point, acceleration response spectrum for the reference site and spectral ratio)

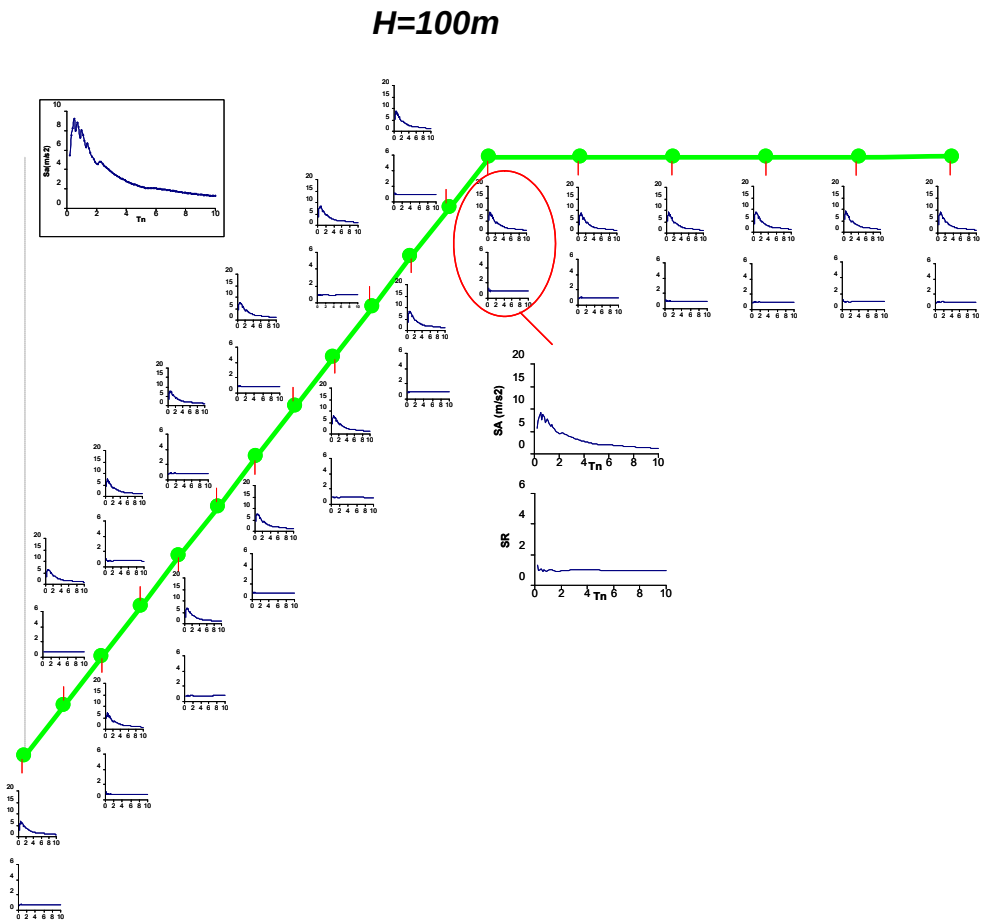

More critical point in empty valleys:

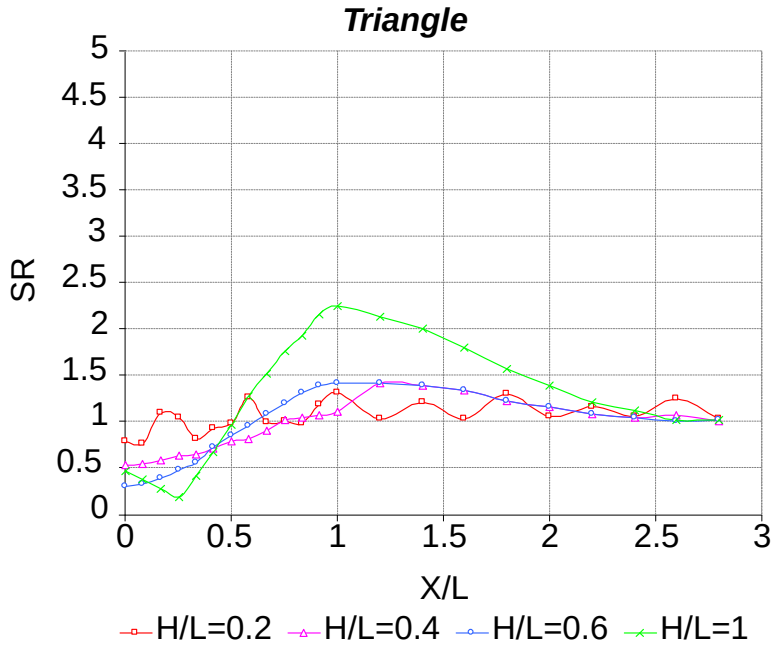

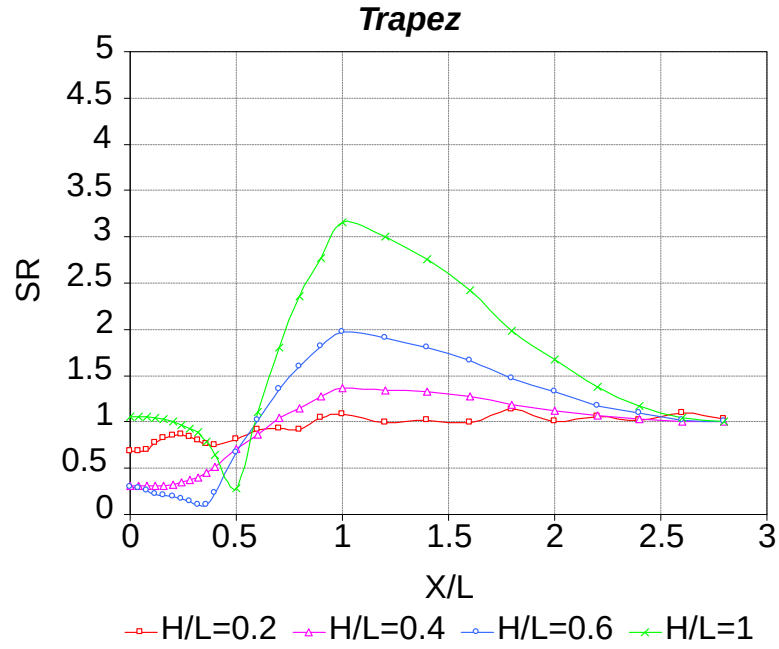

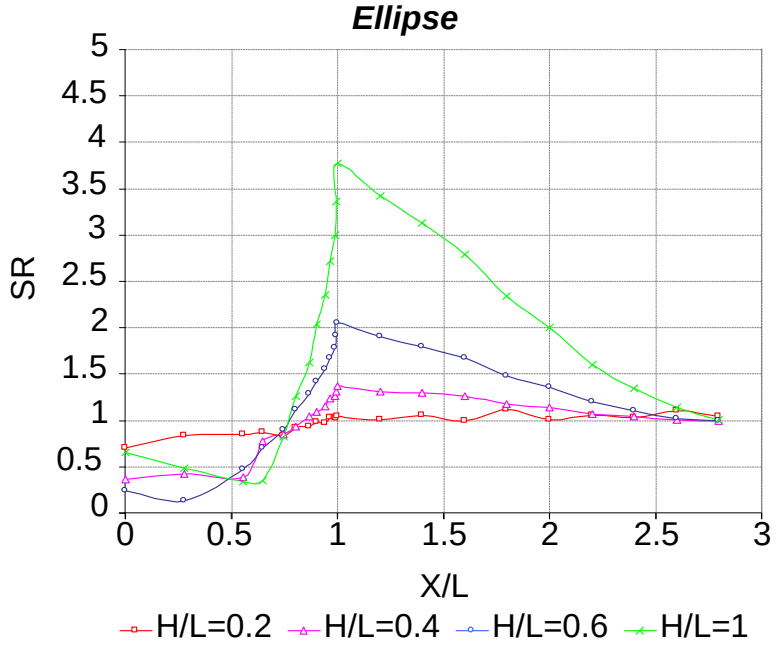

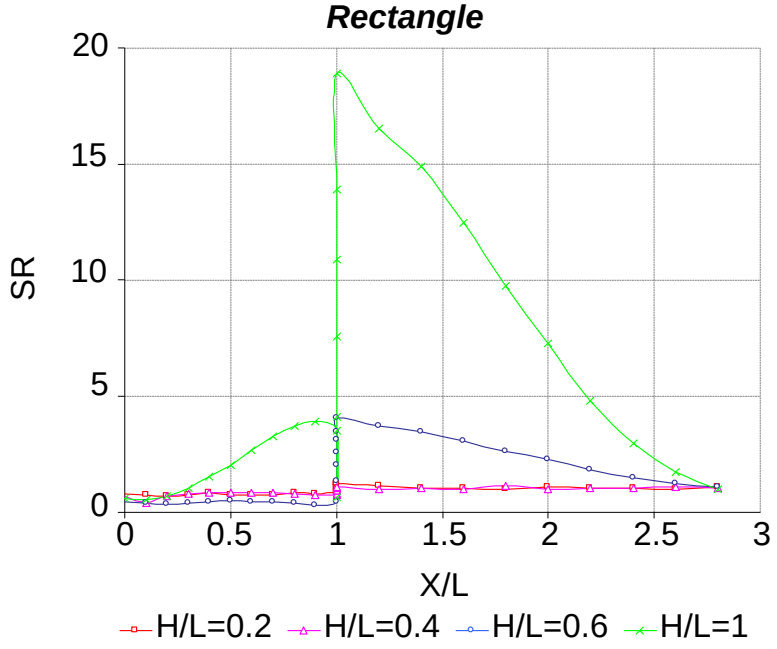

Domain of influence of topographical effects in empty valleys

- If all the acceleration response spectrum curves of the different points of valleys are drawn on a single figure, the domain of influence of topographical effects in empty valleys can be determined:

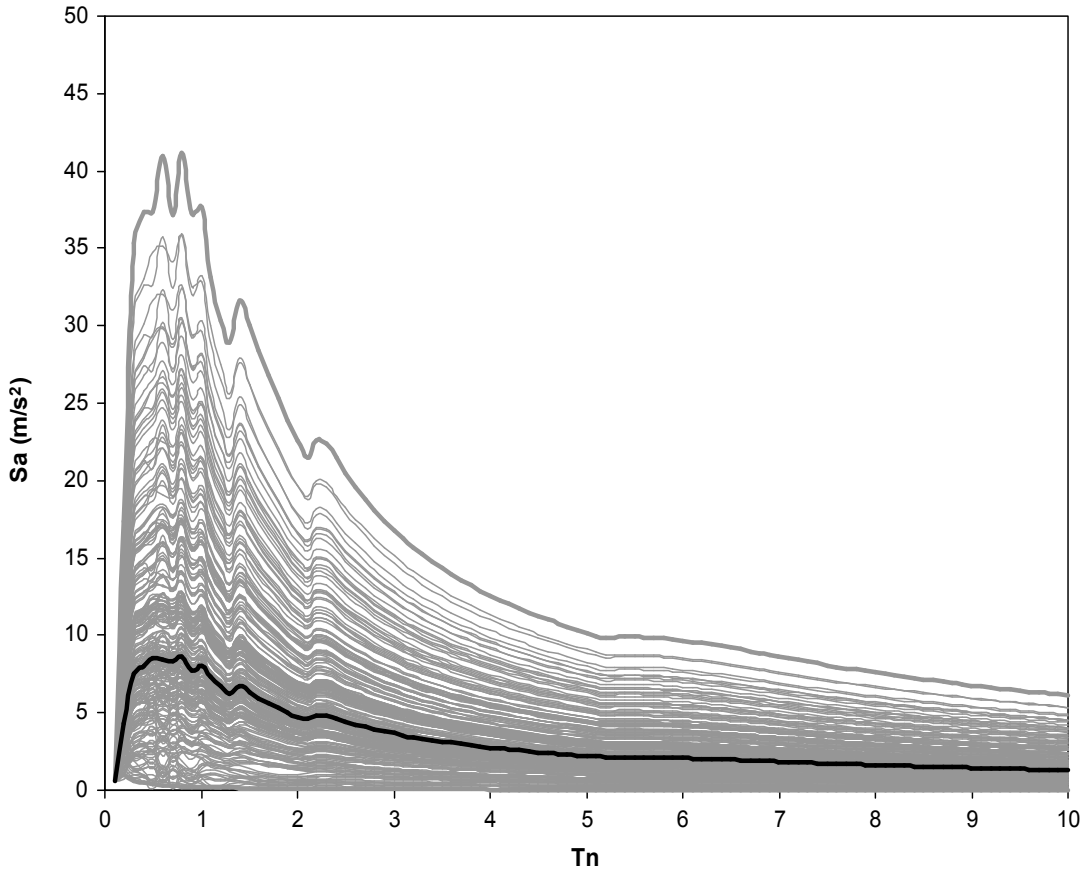

New criterion for empty valleys

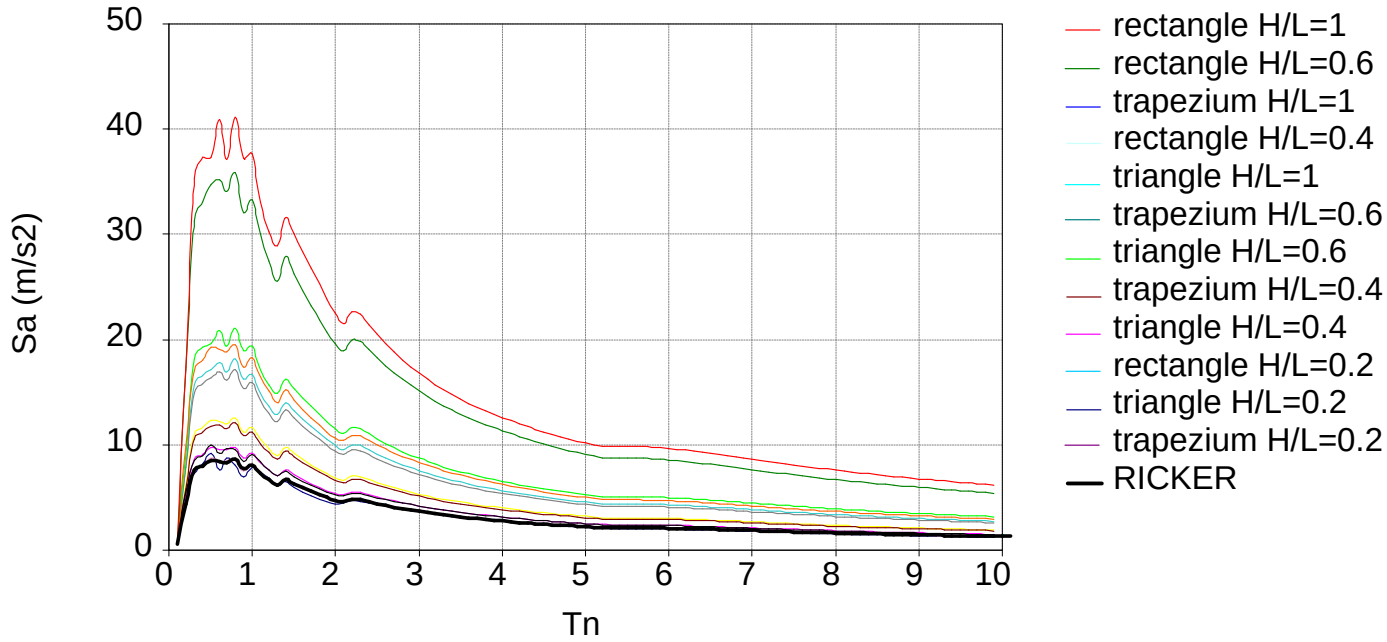

Classification	Figure	Dimension (H/L)	Surface (S) (m^2)	Angle (A)	S/A
1	Rectangle	1	20, 000	90°	222.2
2	Rectangle	0.6	12, 000	90°	133.3
3	Trapezium	1	14, 000	120°	116.7
4	Rectangle	0.4	8, 000	90°	88.8
5	Triangle	1	10, 000	135°	74.07
6	Trapezium	0.6	8, 400	135°	62.2
7	Triangle	0.6	6, 000	150°	40.0
7	Trapezium	0.4	5, 600	146°	38.4
8	Triangle	0.4	4, 000	158°	44.4
8	Rectangle	0.2	4, 000	90°	25.3
9	Triangle	0.2	2, 000	169°	17.3
9	Trapezium	0.2	2, 800	162°	11.8

New criterion for empty valleys

Non-curved geometries (triangle, trapezium and rectangle)

Classification	Figure	Dimension (H/L)	Surface (S) (m^2)	Angle (A)	S/A
1	Rectangle	1	20,000	90°	222.2
2	Rectangle	0.6	12,000	90°	133.3
3	Trapezium	1	14,000	120°	116.7
4	Rectangle	0.4	8,000	90°	88.8
5	Triangle	1	10,000	135°	74.07
6	Trapezium	0.6	8,400	135°	62.2
7	Triangle	0.6	6,000	150°	40.0
7	Trapezium	0.4	5,600	146°	38.4
8	Triangle	0.4	4,000	158°	44.4
8	Rectangle	0.2	4,000	90°	25.3
9	Triangle	0.2	2,000	169°	17.3
9	Trapezium	0.2	2,800	162°	11.8

- The response spectrum curves are independent of the shape of the valley.
- There is a very clear correlation between the parameter **S/A** (surface/angle) and the classification. It is thus possible to model topographical site effects in the various configurations only by means of that parameter (**S/A**).

New criterion for empty valleys

Curved geometries (ellipse and truncated ellipse)

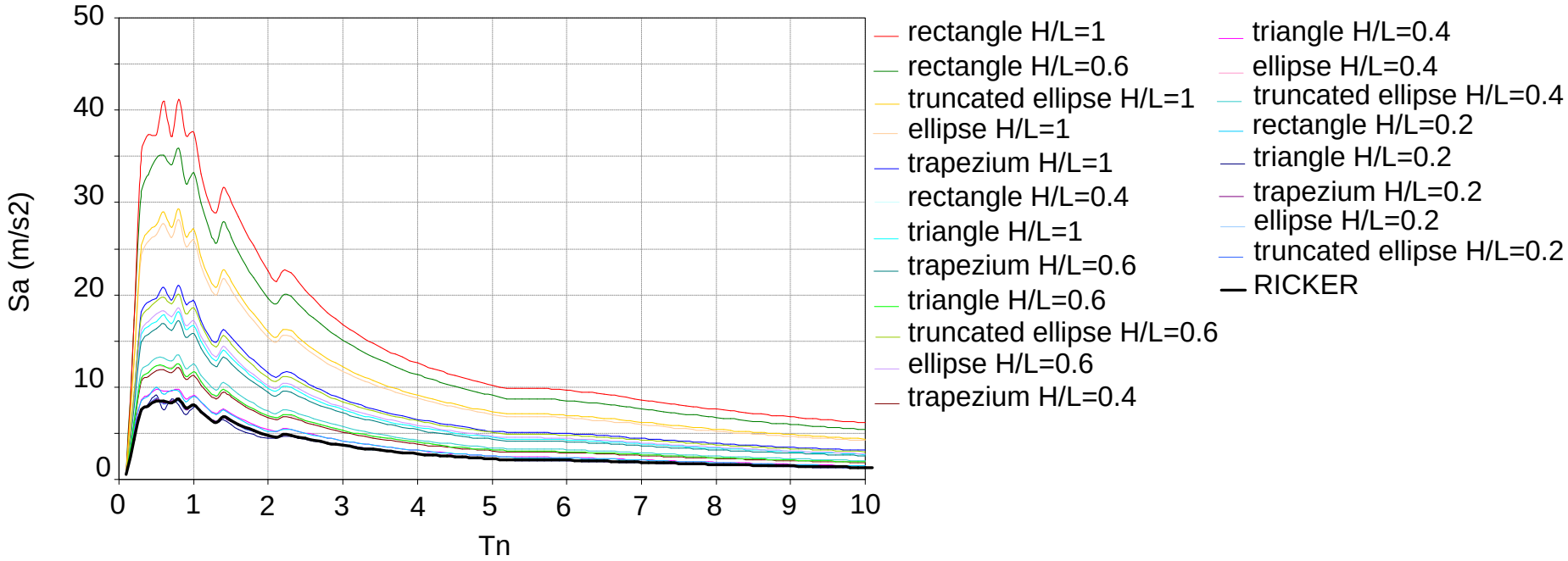

- For every value of H/L, the spectral response increases with the parameter of S/A.
- The behaviour of curved forms (ellipse and truncated ellipse) is intermediate: the spectral curves are always located between those of the rectangular and the trapezoidal valleys.

Parameters of the problem

Geometrical characteristics: Configurations of the studied fully-filled alluvial valleys are triangle, trapezium, rectangle, ellipse and truncated ellipse.

$L = 100$ $L_1/L = 0, 0.4$ $H/L = 0.2, 0.4, 0.6, 1$

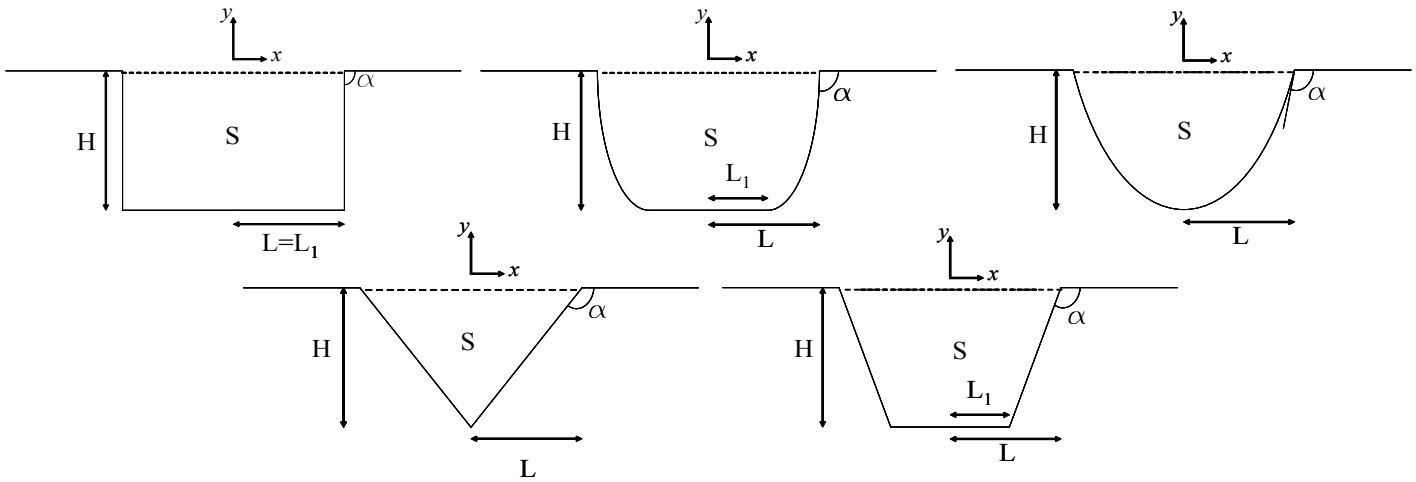

Soil properties:

	E (MPa)	K (MPa)	ν (-)	G (MPa)	ρ (Kg/m^3)	v_S (m/s)	Impedance (α) (-)
Bedrock	6720.0	11200.0	0.4	24.0	2.45×10^3	1000.0	1.0
Sediments	899.5	749.6	0.3	346.0	1.63	465.0	0.3

Seismic solicitation: Vertically incident SV Ricker wave with predominant frequency of 2Hz.

Study of the combined effects in the various fully-filled valleys

- Some geometrical points are chosen as stations
- A triplet of curves is obtained for every chosen observation point and for every type of valley (acceleration response spectrum for each observation point, acceleration response spectrum for the reference site and spectral ratio)

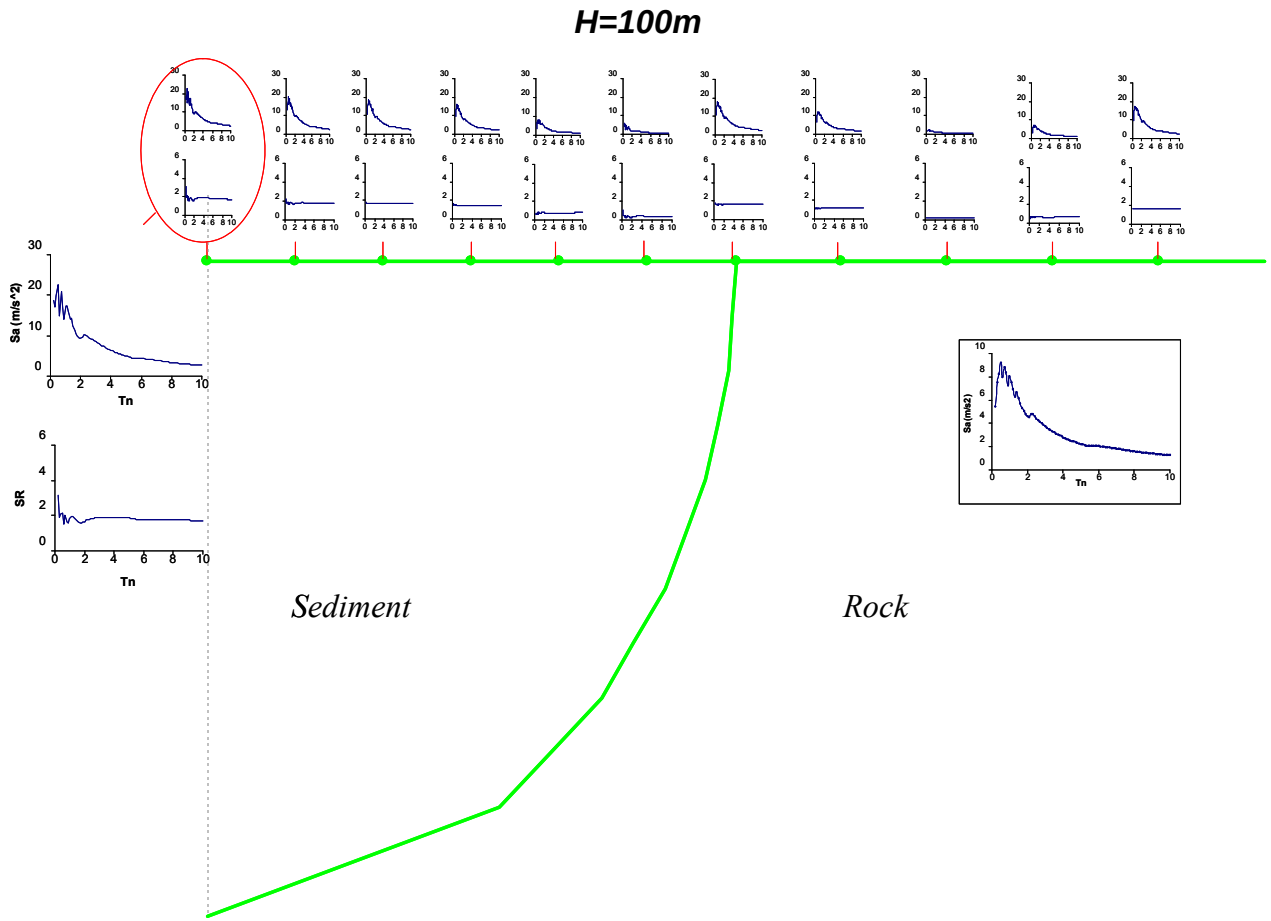

Study of the combined effects in the various fully-filled valleys

- Some geometrical points are chosen as stations
- A triplet of curves is obtained for every chosen observation point and for every type of valley (acceleration response spectrum for each observation point, acceleration response spectrum for the reference site and spectral ratio)

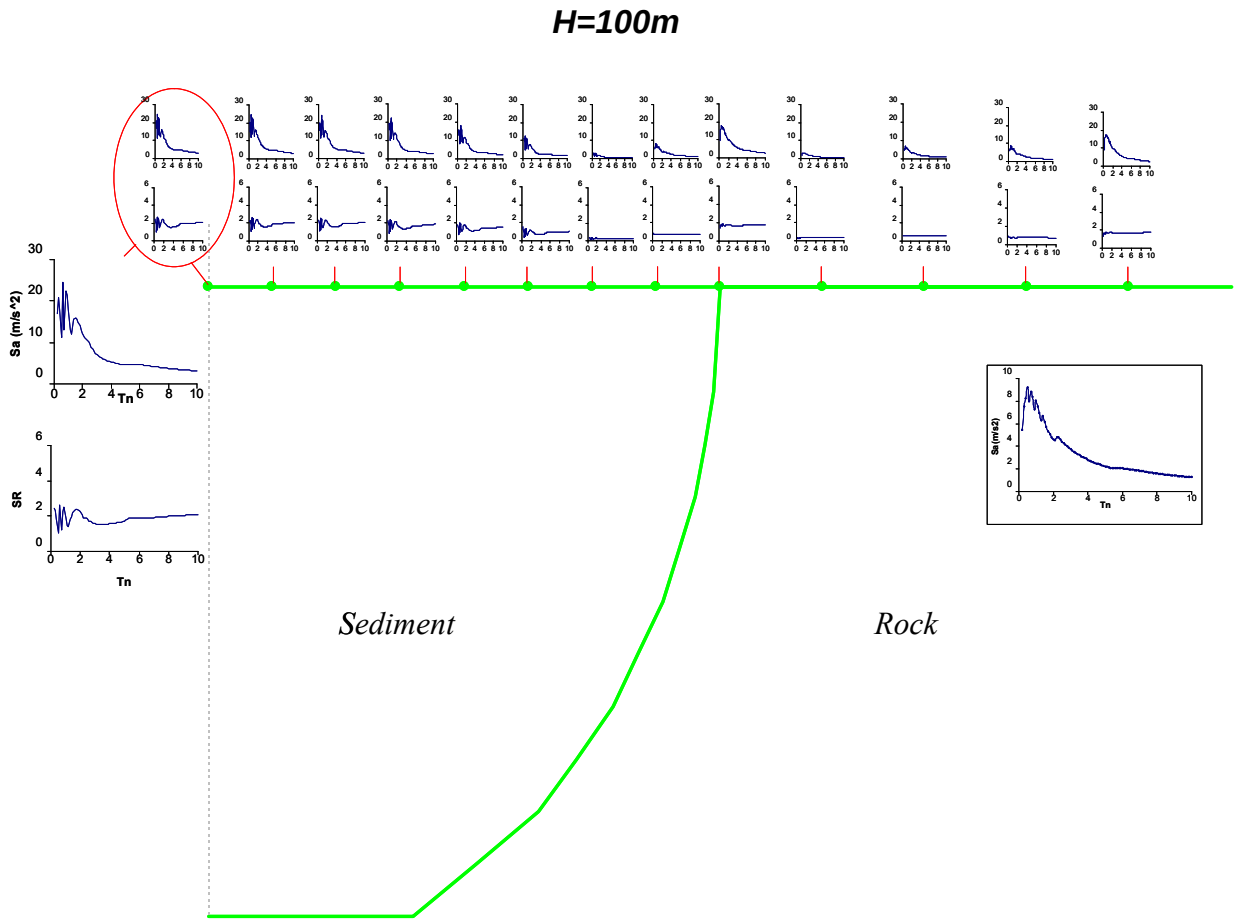

Study of the combined effects in the various fully-filled valleys

- Some geometrical points are chosen as stations
- A triplet of curves is obtained for every chosen observation point and for every type of valley (acceleration response spectrum for each observation point, acceleration response spectrum for the reference site and spectral ratio)

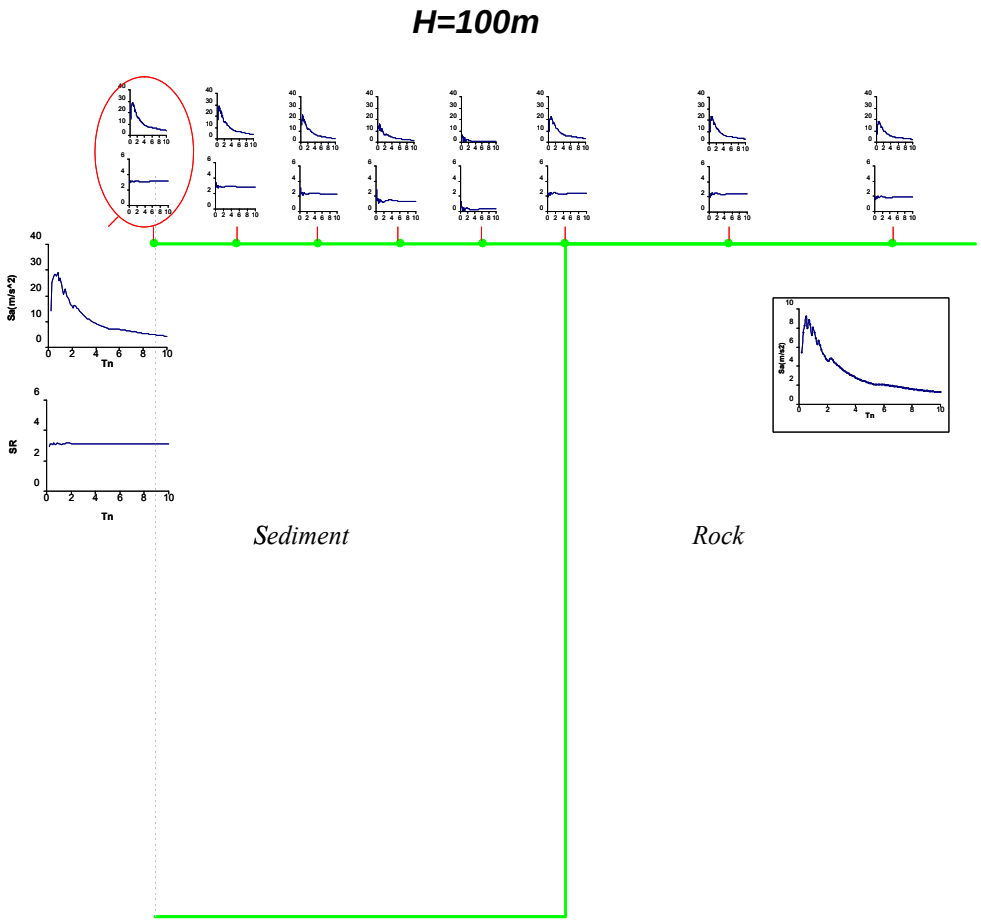

Study of the combined effects in the various fully-filled valleys

- Some geometrical points are chosen as stations
- A triplet of curves is obtained for every chosen observation point and for every type of valley (acceleration response spectrum for each observation point, acceleration response spectrum for the reference site and spectral ratio)

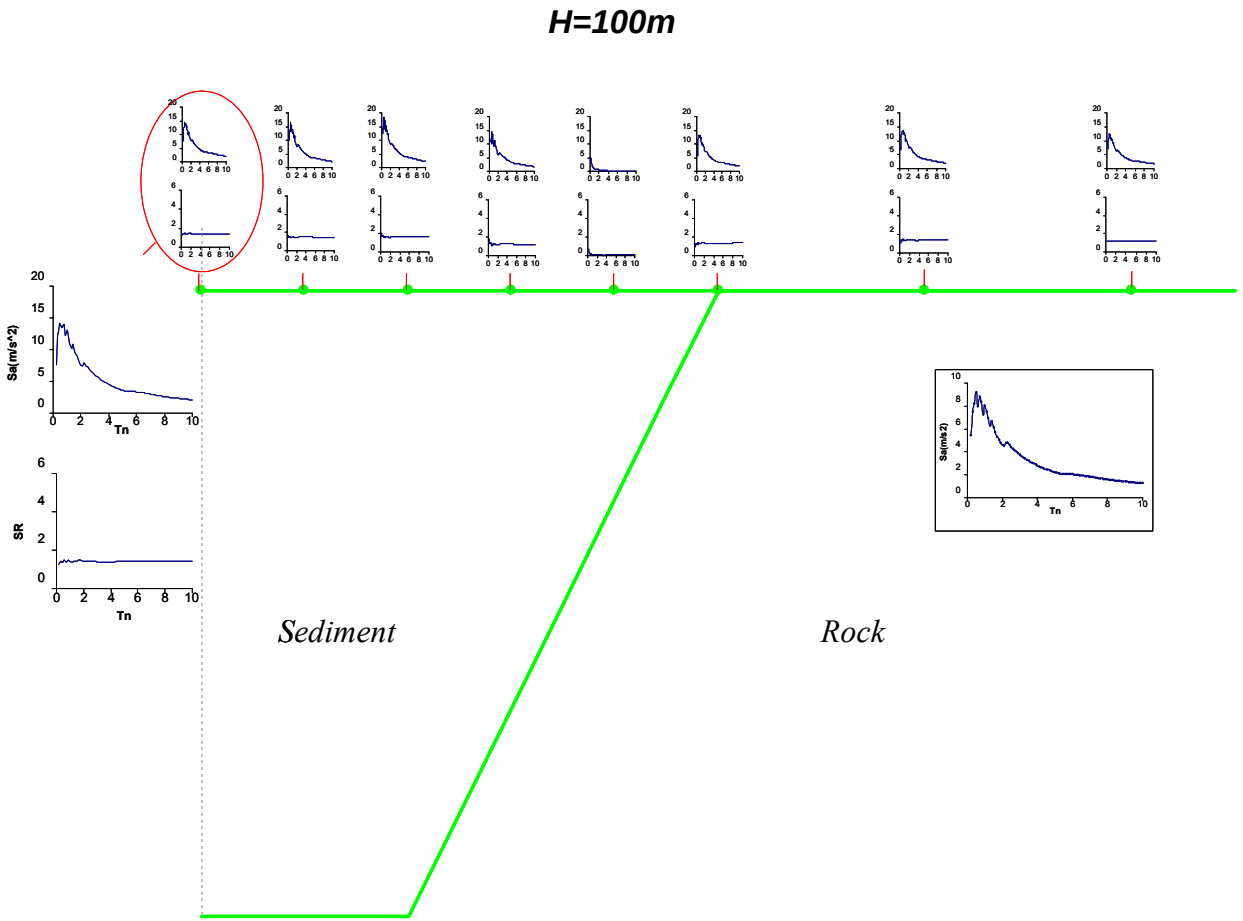

Study of the combined effects in the various fully-filled valleys

- Some geometrical points are chosen as stations
- A triplet of curves is obtained for every chosen observation point and for every type of valley (acceleration response spectrum for each observation point, acceleration response spectrum for the reference site and spectral ratio)

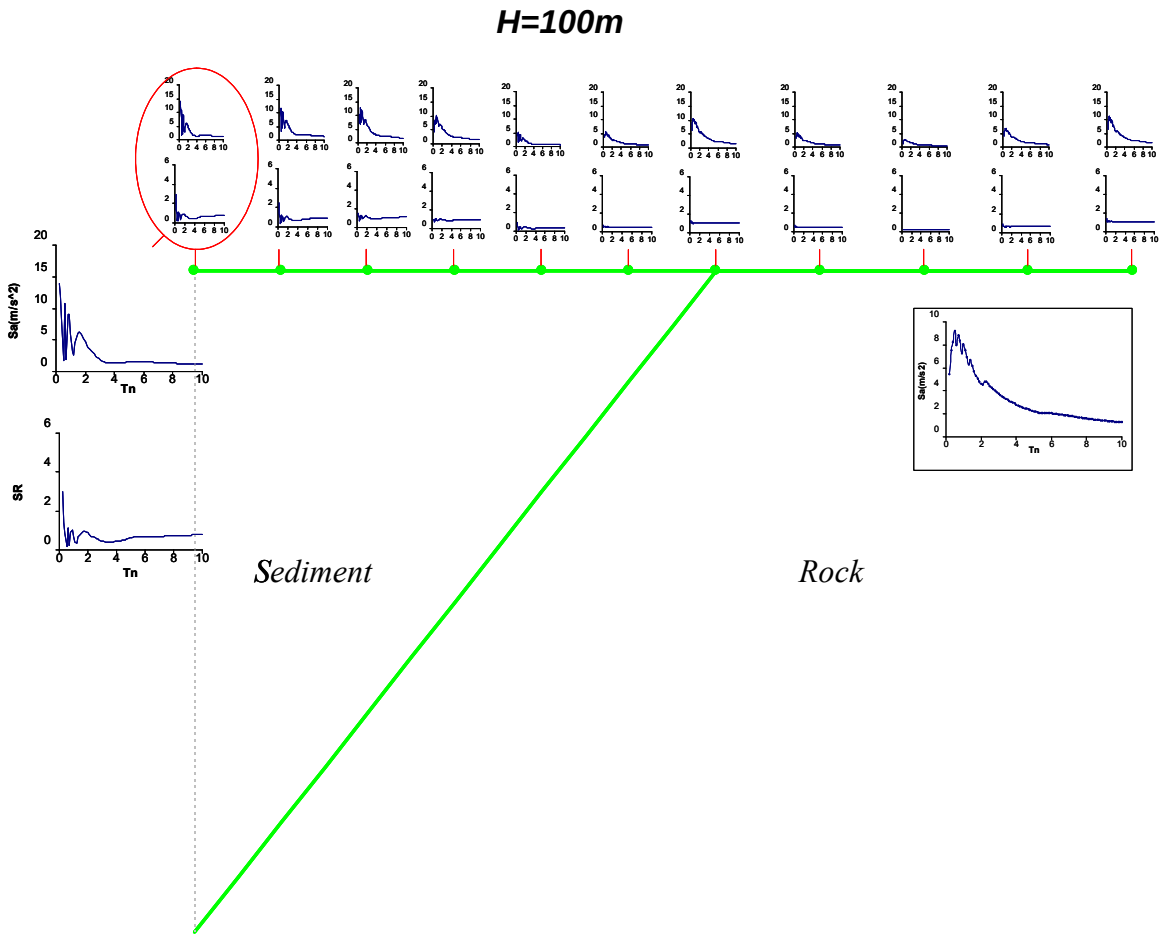

Fully-filled sedimentary valleys

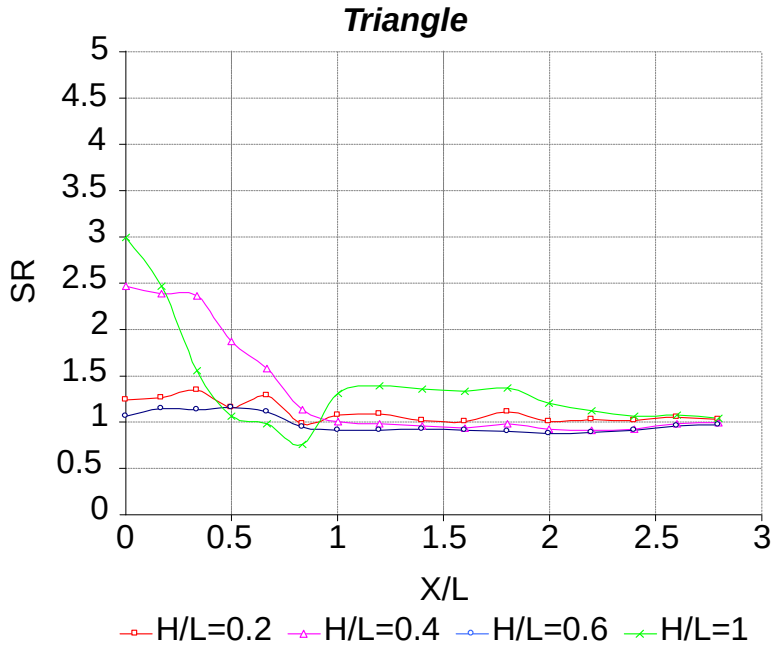

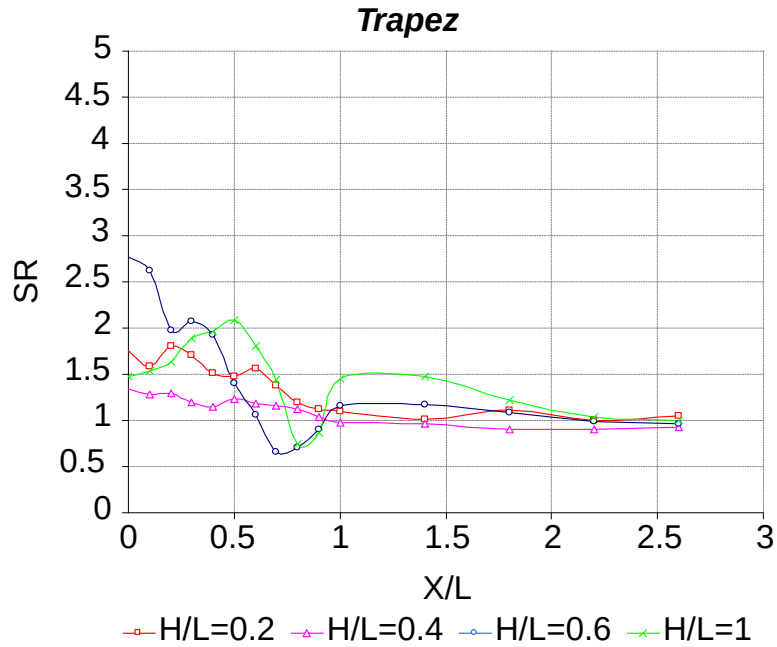

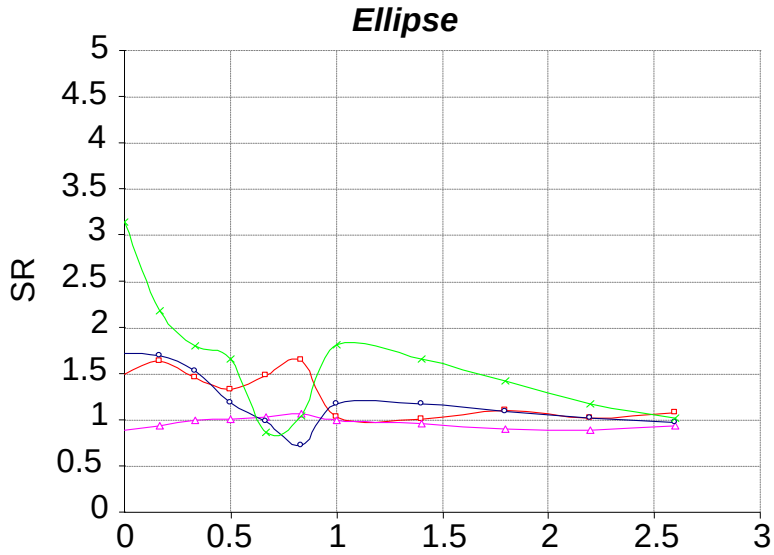

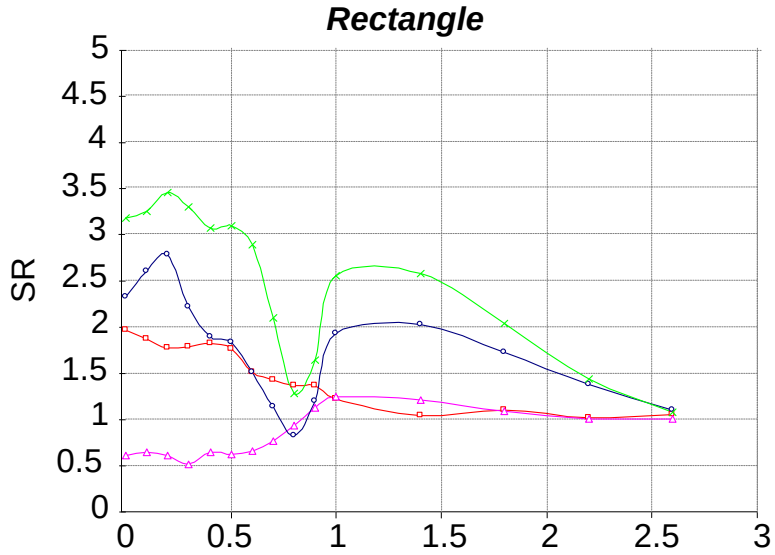

Fully-filled sedimentary valleys

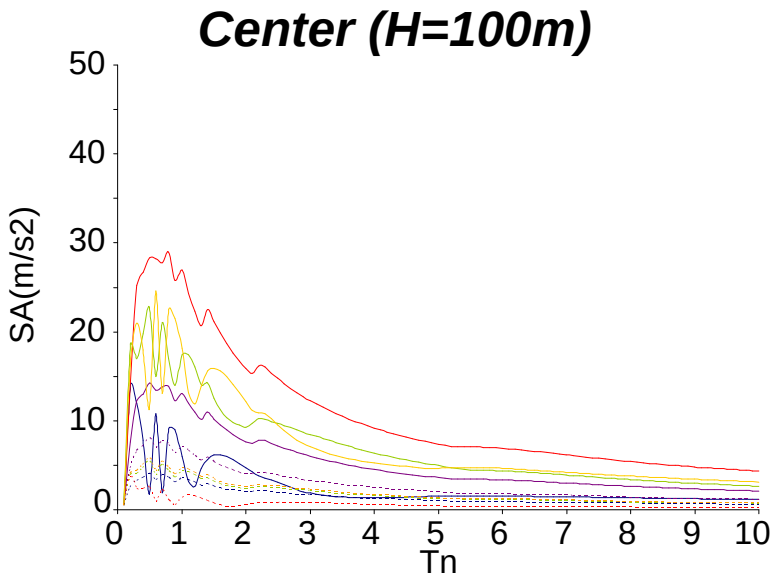

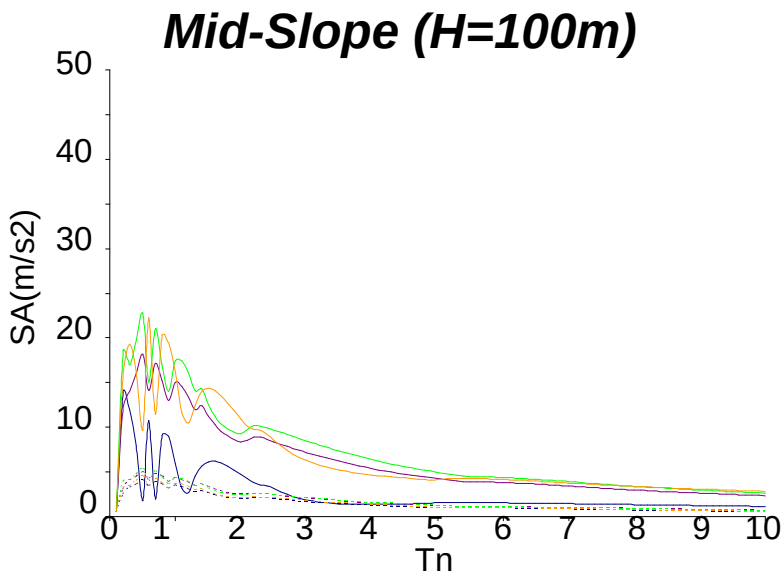

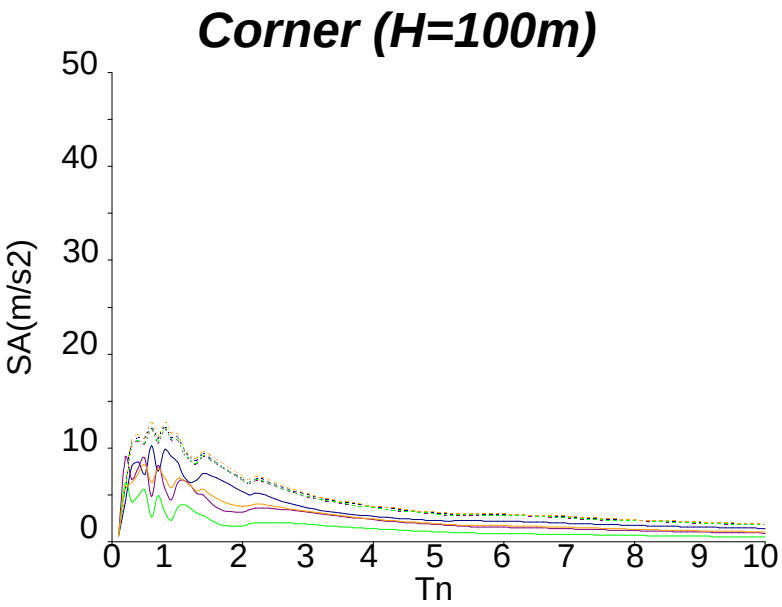

- Central zone
- Lateral zone

Fully-filled sedimentary valleys

In the central zone (from $X/L = 0$ to mid-slope)

- ***Sedimentary effects dominate topographical effects***:
  One-dimensional analysis can be used to estimate the spectral acceleration response of a filled valley if we can not perform 2D analysis.

In the lateral zone (X/L greater than mid-slope)

- The spectral response of the sedimentary valleys can be deduced from the characteristic spectra of topographical effects.

Parameters of the problem

Geometrical characteristics: Configurations of the studied partially-filled alluvial valleys are triangle and trapezium.

$L = 100$ $L_1/L = 0, 0.4$ $H/L = 0.2, 0.4, 0.6, 1$ $H_1/H = 0, 0.25, 0.5, 0.75, 1$

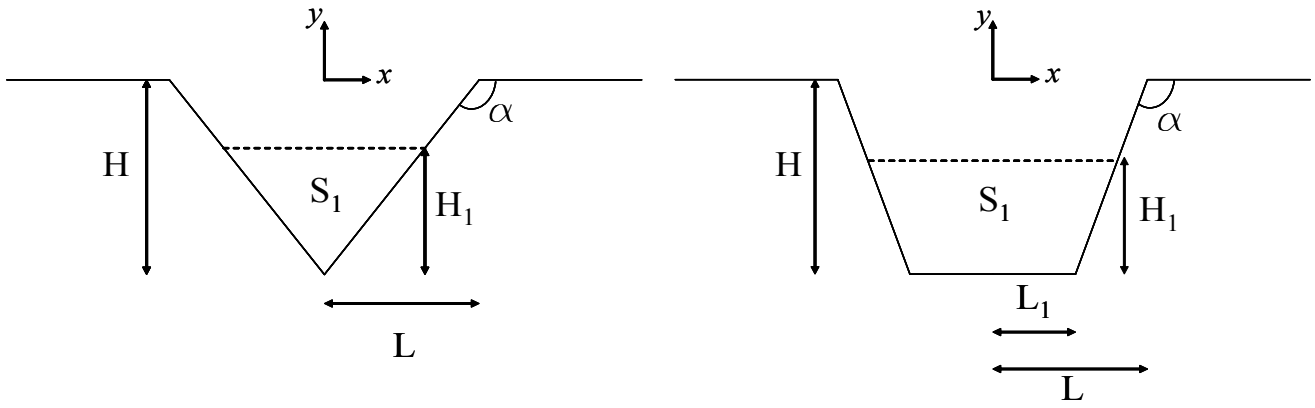

Soil properties:

	E (MPa)	K (MPa)	ν (-)	G (MPa)	ρ (Kg/m^3)	v_S (m/s)	Impedance (α) (-)
Bedrock	6720.0	11200.0	0.4	24.0	2.45×10^3	1000.0	1.0
Sediments	382.0	318.0	0.3	147.0	1.63	300.0	0.2
	899.5	749.6	0.3	346.0	1.63	465.0	0.3
	1527.0	1272.0	0.3	587.0	1.63	600.0	0.4
	2385.0	1988.0	0.3	917.0	1.63	750.0	0.5

Seismic solicitation: Vertically incident SV Ricker wave with predominant frequency of 2Hz.

Alluvial valleys: Spatial evolution

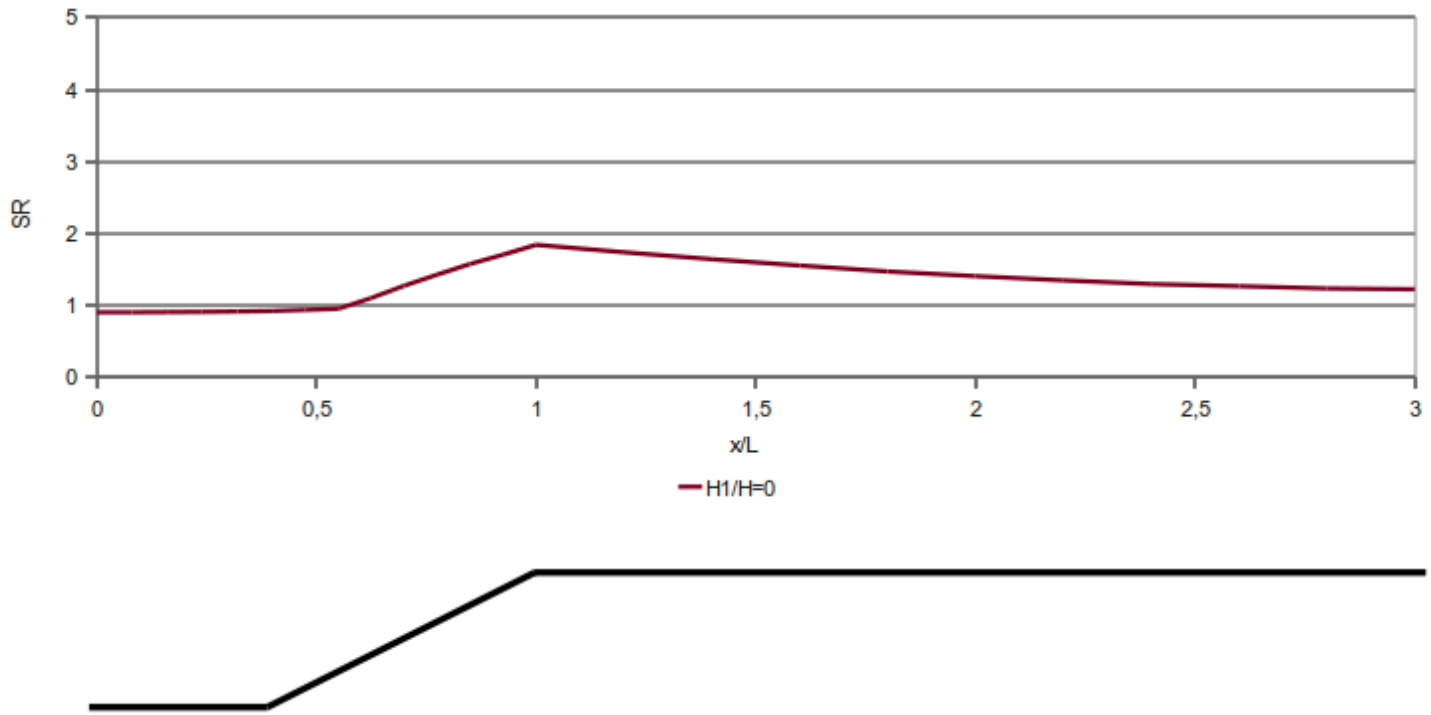

Trapezoidal valley: $H/L = 0.6$ **-** $\alpha = 0.3$

- Empty valley : Maximum amplification at the edge of the valley
- Fully-filled valley : Maximum amplification at the centre of the valley

Alluvial valleys: Spatial evolution

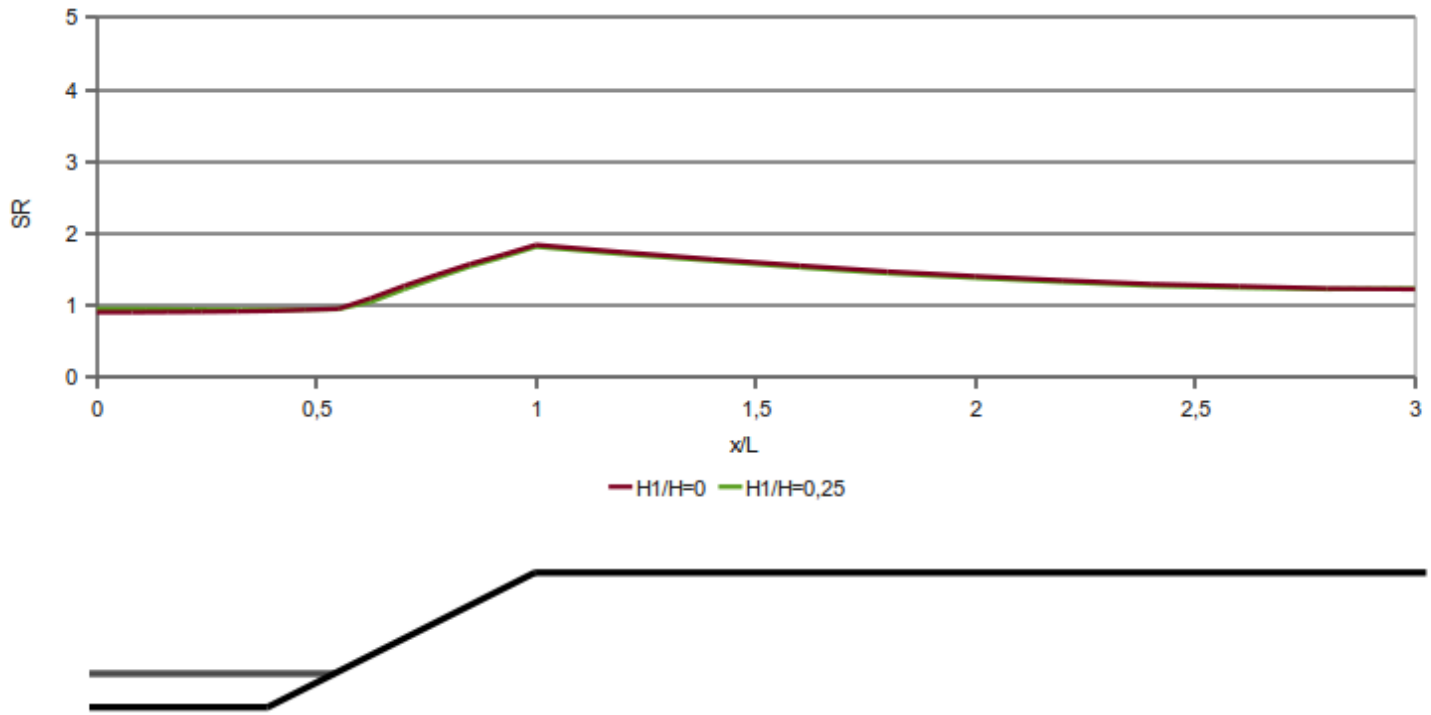

Trapezoidal valley: $H/L = 0.6$ **-** $\alpha = 0.3$

- Empty valley : Maximum amplification at the edge of the valley
- Fully-filled valley : Maximum amplification at the centre of the valley

Alluvial valleys: Spatial evolution

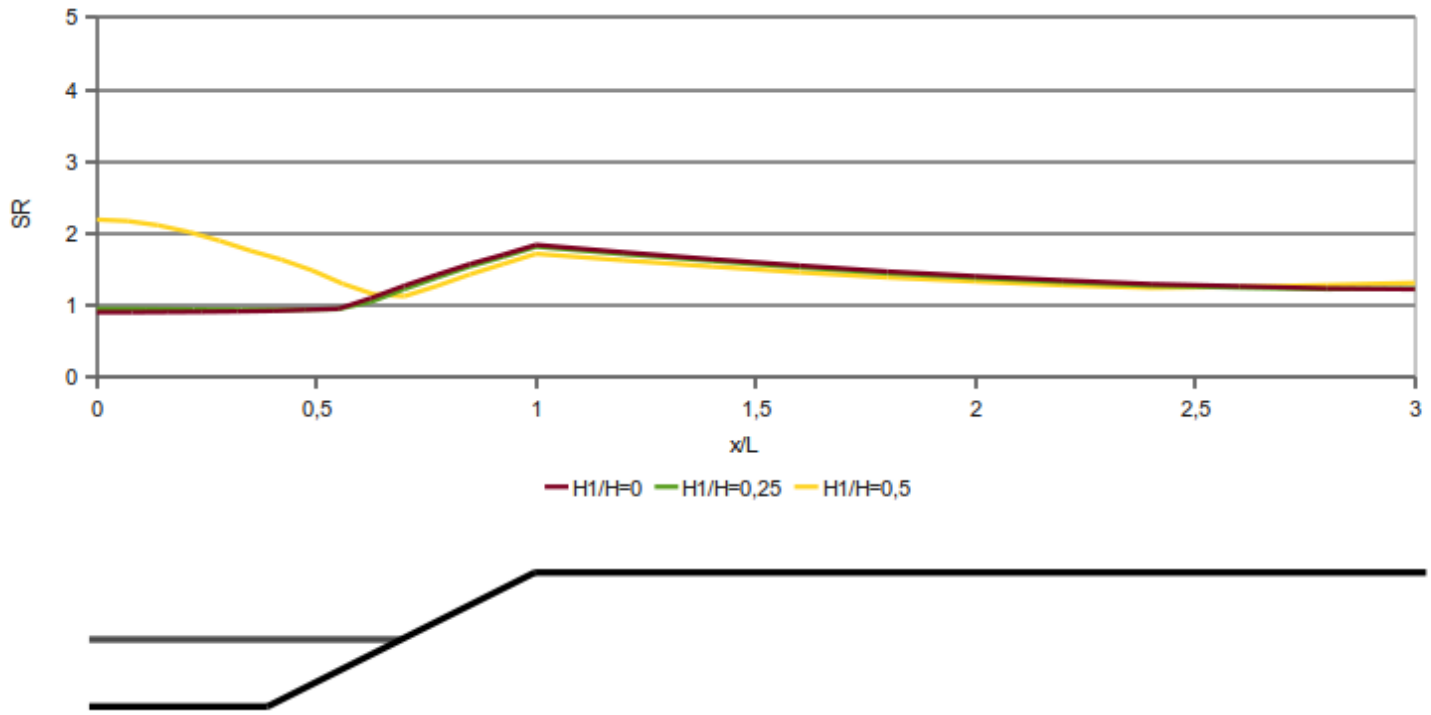

Trapezoidal valley: $H/L = 0.6$ **-** $\alpha = 0.3$

- Empty valley : Maximum amplification at the edge of the valley
- Fully-filled valley : Maximum amplification at the centre of the valley

Alluvial valleys: Spatial evolution

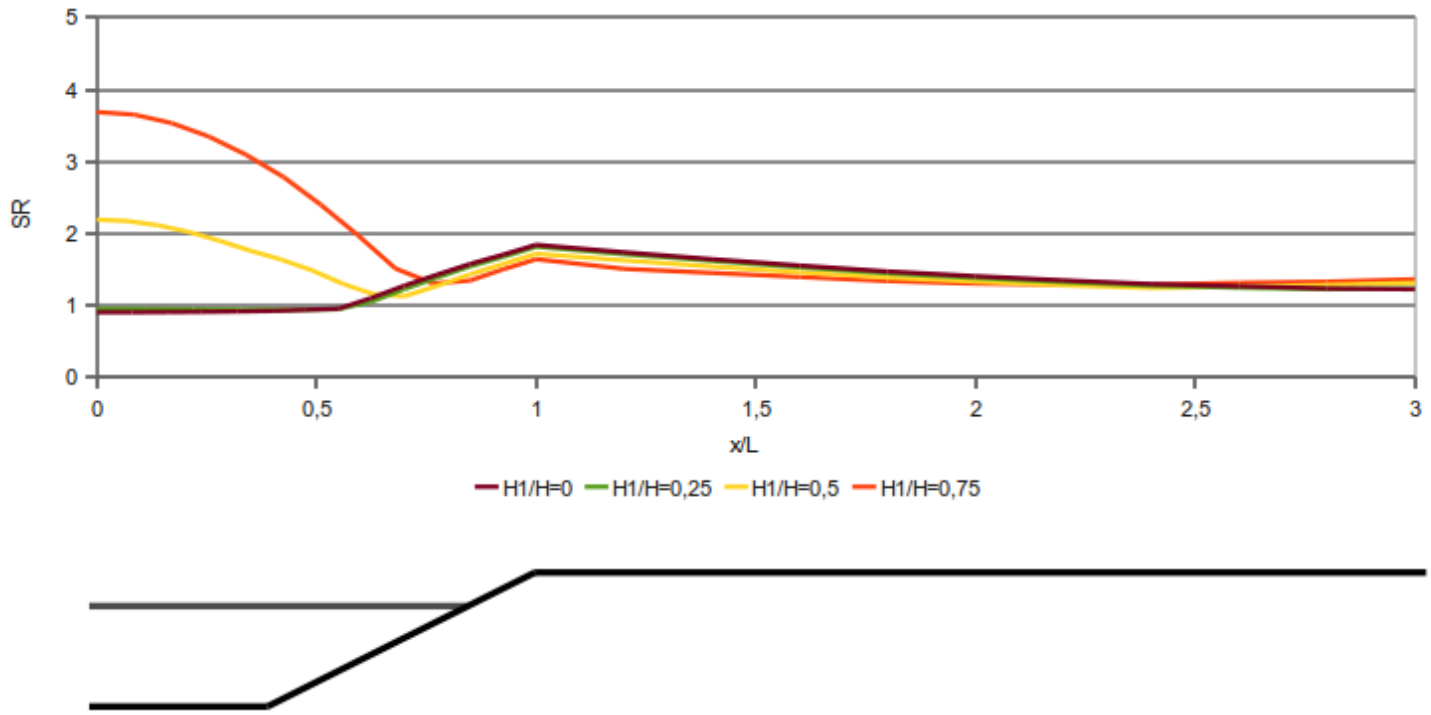

Trapezoidal valley: $H/L = 0.6$ **-** $\alpha = 0.3$

- Empty valley : Maximum amplification at the edge of the valley
- Fully-filled valley : Maximum amplification at the centre of the valley

Alluvial valleys: Spatial evolution

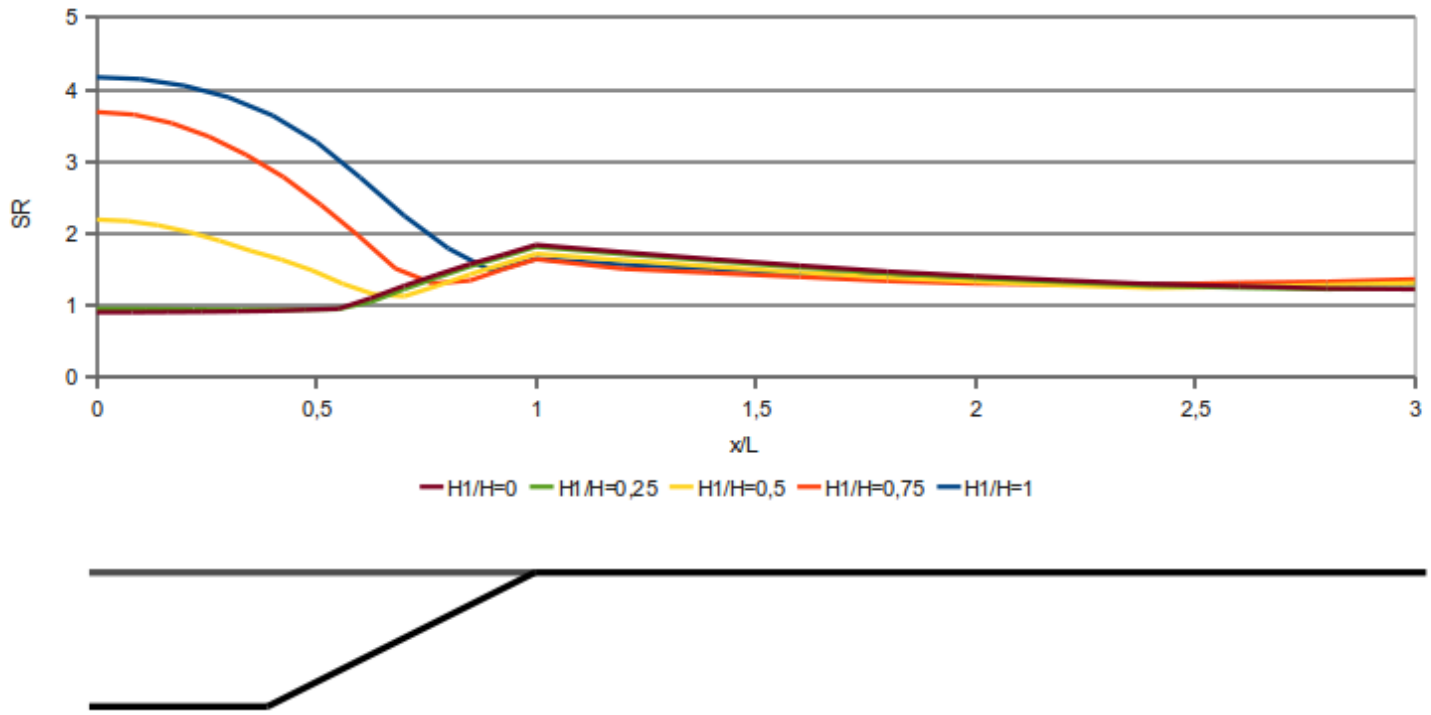

Trapezoidal valley: $H/L = 0.6$ **-** $\alpha = 0.3$

- Empty valley : Maximum amplification at the edge of the valley
- Fully-filled valley : Maximum amplification at the centre of the valley

Spectral ratio *SR*

Triangular valleys

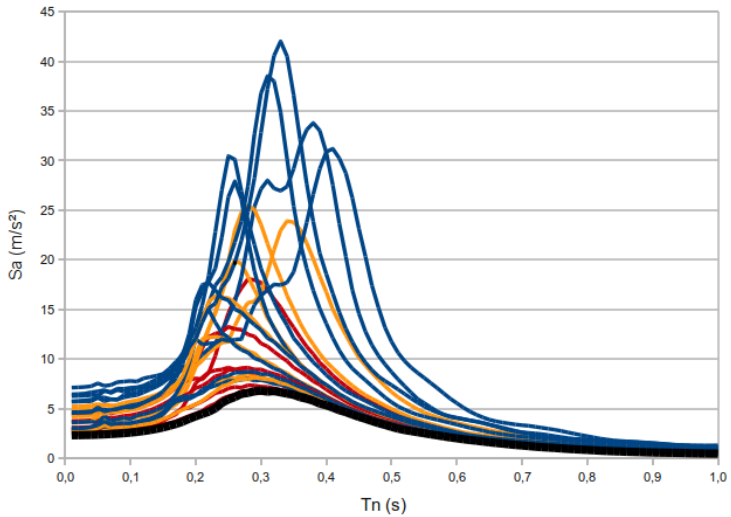

Trapezoidal valleys

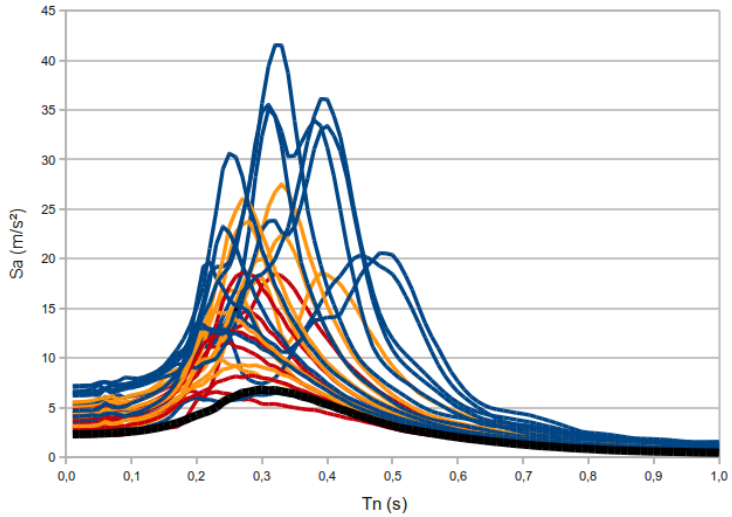

Black : Ricker - Red : $\alpha = 0.4$ ***- Yellow :*** $\alpha = 0.3$ ***- Blue :*** $\alpha = 0.2$

$\alpha \downarrow \Longrightarrow$ **Amplitude of spectra increases**

Site period T_s

Parameter $\dfrac{S_1}{\alpha\sqrt{\alpha}}$

$$13\,000 \leqslant \frac{S_1}{\alpha\sqrt{\alpha}} \leqslant 120\,000$$

$\alpha = 0,3$ / H (m)	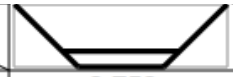	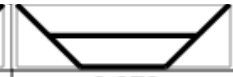	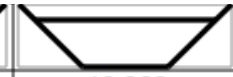	
20	2 752	6 373	10 863	16 222
40	5 504	12 746	21 726	32 445
60	8 256	19 119	32 590	48 667
100	3 621	14 484	32 590	57 937

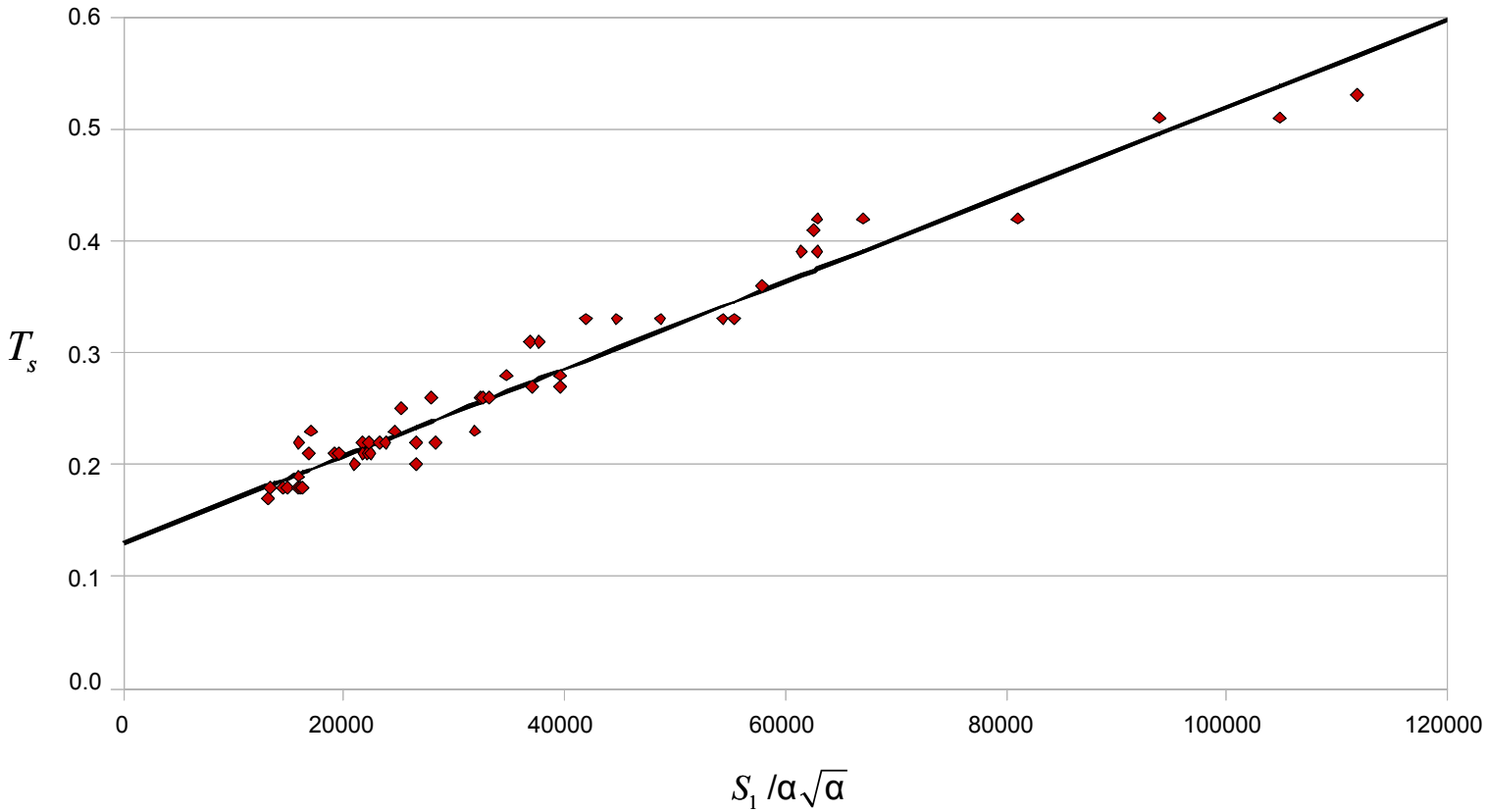

Evolution of spectral ratio

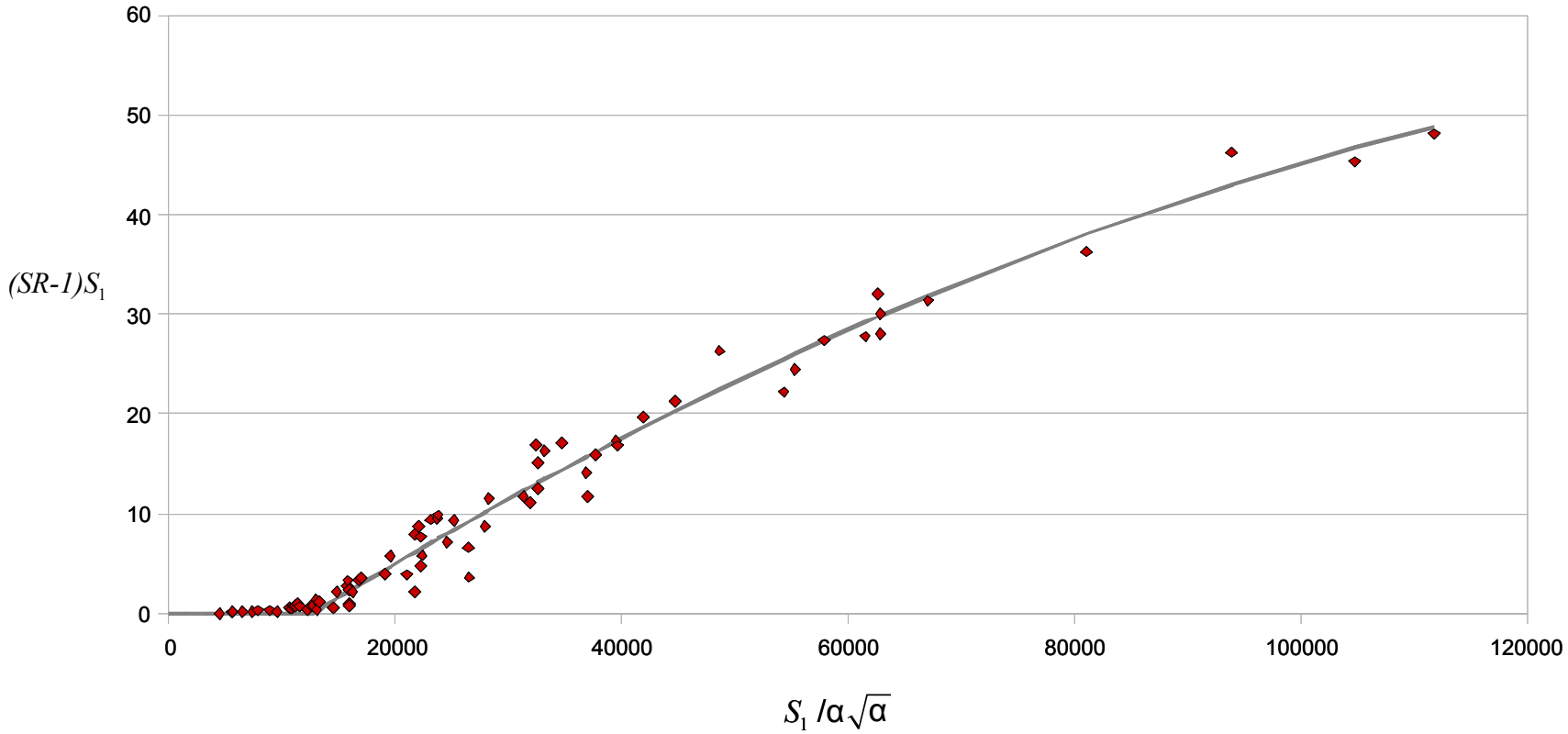

1 Unsaturated soils
- General context and fields of application
- Basic assumptions
- Governing equations

2 Boundary element method
- Problematics
- Fundamental Solution
- Boundary Integral Equation
- Discretization

3 Implementation in « HYBRID » FEM/BEM code
- Programming
- Validation

4 Applications in seismic site effects
- Introduction
- Topographic site effects in 2D configurations
- Combined effects in fully-filled alluvial valleys
- Alluvial effect in a partially-filled valley

5 **Conclusion and Perspective**

Summary

- The developments of the BEM for unsaturated soils carried out during this thesis are based on the thermo-hydro-mechanical (THHM) and hydro-mechanical (HHM) models. These phenomenological models are based on poromechanical theory and experimental observations, and were obtained within the framework of the suction-based mathematical model presented by Gatmiri (1997) and Gatmiri et al. (1998).
- We establish for the first time the boundary integral equations (BIE) and the associated fundamental solutions for unsaturated porous media subjected to
  - Isothermal quasi-static loading: 2D in the Laplace transform domain [Maghoul et al. BeTeq (2010)],
  - Non-isothermal quasi-static loading: 2D and 3D in Laplace transform and time domain [Gatmiri et al. IJSS (2010), Maghoul et al. IJNAMG (2010)],
  - Dynamic loading: 2D and 3D in the Laplace transform domain [Maghoul et al. SDEE (2010), Maghoul et al. ECCM (2010)].
- The BE formulations based on the CQM concerning saturated and unsaturated porous media subjected to isothermal quasi-static and dynamic loadings are implemented via the computer code "HYBRID" [Maghoul et al. JMM (2010)].
- Parametric studies on seismic site effects are carried out. The aim is to achieve a simple criterion directly usable by engineers, combining the topographical and geological characteristics of the soil, to predict the amplification of acceleration response spectra in both sedimentary and hollow valleys [Gatmiri, Maghoul & Arson SDEE (2009), Gatmiri, Maghoul & LePense JMM (2010)].

Prospects

- Studying the numerical stability of the BEM formulations based on the convolution quadrature method (CQM) established for wave propagation as well as for consolidation problems in saturated and unsaturated porous media.
- Considering the suction effect on displacement, water pressure and air pressure responses of unsaturated soil subjected to quasi-static and dynamic loadings.